Ocean Wave Simulation and Prediction

Sihan Yu

Thesis submitted to the faculty of the
Virginia Polytechnic Institute and State University
in partial fulfillment of the requirements for the degree of

Master of Science
in
Computer Engineering

Yaling Yang, Chair
Majid Manteghi
Carl B. Dietrich

August 6, 2018
Blacksburg, Virginia

Keywords: Ocean Wave Simulation, Ocean Wave Prediction, Ocean Wave Spectrum, Fast Fourier Transform, Neural Network, Multiple Linear Regression, Oscillation Measurement

Ocean Wave Simulation and Prediction

Sihan Yu

ABSTRACT

WiFi can provide network coverage for users on land at anytime and anywhere, but on the sea, the wireless communication scenes change dramatically due to the signals are non-existence. Although some techniques (e.g. satellite, undersea fiber, microwave communication) have been used in marine communication, they are either too expensive with very small bandwidth, or too limited in its coverage range. We propose to develop a marine wireless mesh network which is formed by low cost buoyed wireless base stations to provide broadband connectivity for users on the sea.

Ocean wave simulation and prediction are key technologies in developing marine mesh network, because marine environments are dramatically different from terrestrial environments. The ocean waves have characteristics of rhythmic oscillations and the line of sight between two communication nodes is often blocked by them. Therefore, we have to develop a new wave-state-aware networking protocol which is suitable for marine environments. Ocean wave simulation technology can simulate this kind of dynamic environments and provide a test platform for the development of marine mesh network. Ocean wave prediction technology can improve the throughput of marine wireless network. Thus, they are indispensable technologies in developing marine mesh network.

In this thesis, we designed an ocean wave measurement method, two ocean wave prediction methods, and an ocean wave simulation method.

Firstly, we designed an accelerometer-based ocean wave measurement method. It can measure the real time wave height accurately.

Secondly, we designed an Elman-neural-network-based ocean wave prediction method for nonlinear waves. It has a higher prediction accuracy than other neural network methods in nonlinear wave prediction.

Thirdly, we designed a multiple-linear-regression-based ocean wave prediction method for linear waves. It has a higher prediction accuracy and less time consumption than other methods in linear wave prediction.

Finally, we implemented and improved a spectrum-based ocean wave simulation method which is originally proposed by Tessendorf. It can present the movement of ocean waves realistically and in real time.

To sum up, above four methods provide an effective test platform and technical support for the development of our marine mesh network.

Ocean Wave Simulation and Prediction

Sihan Yu

GENERAL AUDIENCE ABSTRACT

With the development of wireless communication technology, WiFi has been an indispensable resource for daily work and pleasure. However, in the marine environments, WiFi is not exist. Thus, passengers and workers on the sea are eager for it. We propose to develop a marine wireless mesh network which is formed by low cost buoyed wireless base stations to provide WiFi for users on the sea.

Marine environments are dramatically different from terrestrial environments. The ocean waves have characteristics of rhythmic oscillations and the link between two buoys is often blocked. Therefore, the signals are also intermittent. We decided to develop a new wave-state-aware networking protocol to eliminate the harmful effect of this kind of rhythmic oscillations. Ocean wave simulation and prediction are key technologies in developing networking protocol, in which ocean wave simulation technology can simulate the marine environments and provide a test platform for developing networking protocol. Ocean wave prediction technology can improve the network throughput. Thus, they are indispensable technologies in developing marine mesh network.

In this thesis, we mainly research three problems that related to ocean waves, they are ocean wave measurement, ocean wave prediction and ocean wave simulation. Ocean wave measurement can tell us the current wave height of a buoy, ocean wave prediction can tell us the future height of a buoy, after we know these information, we can decide whether allow the buoy to send signal. It can not only save energy, but also improve the success rate of communication. Ocean wave simulation can provide us a dynamic environment to test whether our networking protocol works well.

To sum up, these methods provide an effective test platform and technical support for the development of our marine mesh network.

Acknowledgments

My master's journey at Virginia Tech is a precious experience in my life. It gives me the opportunity to work with excellent teachers and students and enjoy beautiful campus. Here, I want to express my gratitude to many people.

First of all, I want to thank my advisor, Professor Yaling Yang. She provides me with an opportunity to pursue my dream on such a high-level stage. Professor Yang's wisdom and insight leave a deep impression on me. She not only gives me meticulous guidance, but also provides me with financial support, so that I can pursue my dream without worries. Under her guidance, my academic level was greatly improved in the past two years.

Secondly, I would like to thank my committee members, they are Professor Majid Manteghi and Professor Carl B. Dietrich. Thank them for acting as my defense committee members, and also thank them for their valuable comments on my thesis.

Thirdly, I would like to thank the students in our lab. Kexiong Zeng provides a lot of help during my study. Sihao Sun often discusses issues with me and I really benefit from him. In addition, I would also like to thank other students like Yanzhi Dou, He Li and Yousi Lin for their help in my study and life. I miss the time we spent together.

Finally, I would like to thank my parents. They have been my strongest support. With them in my life, I will never be driven into a corner. Their selfless and consistent support allows me to face all difficulties with calm and dignity.

Contents

List of Figures

List of Tables

Chapter 1 Introduction

Ocean wave simulation and prediction are widely used in fields of computer graphics, ocean engineering, fluid mechanics, etc. This chapter mainly introduces the background and motivation of our research. First, we introduce the research background and related concepts of ocean wave simulation and prediction. Then, we introduce motivation and content of our research project. Finally, we conclude our contributions and the structure of this thesis.

1.1 Background

In this section, we introduce some related concepts, application fields and technical difficulties of ocean wave simulation and prediction.

1.1.1 Ocean Wave Simulation

The ocean wave simulation in this thesis refers to using computer to show the movement of ocean waves. This technology is widely used in special effects of film, 3D games, simulated training of navigation, reconstruction of ocean battlefield environment, etc [Fre08]. The difficulty of ocean wave simulation lies in ensuring the reality as well as the real time performance of animation [Hu06]. However, they are a pair of contradictory evaluation indicators, because if you want to ensure the reality of animation, you have to use a more complex mathematical model to generate the animation, this process will inevitably take more time so that cannot guarantee the fluency of animation. In practical applications, there is usually a trade-off between reality and real time performance according to different application scenarios and requirements.

1.1.2 Ocean Wave Prediction

The ocean wave prediction in this thesis refers to predicting the oscillation mode of a certain point on the sea surface, rather than predicting the sea state of a wide sea area in the sense of meteorology. The most common application of this technology is to predict the motion of ships

[Gir10], because ships are float on the sea, predicting the oscillation mode of sea surface is the basis of predicting the motion of ships. This technology is of great significance and widely used in military and civilian fields, e.g. to ensure the taking-off and landing safety of carrier-based aircraft; to improve the performance of ship-borne weapons [Kha05]; to provide data support for structure design of harbors and ships [Gop15].

1.2 Motivation

This section mainly introduces our motivation of conducting ocean wave simulation and prediction. We propose to construct a Marine Mesh Network (MMN, as shown in Figure 1.1) to provide WiFi for tourists and drilling platforms on the sea. Ocean wave simulation and prediction can not only provide a test platform for the design of MMN, but also improve the performance of MMN. Subsection 1.2.1 mainly introduces our research project, i.e. the structure and technical details of MMN. Subsection 1.2.2 and 1.2.3 introduce the role of ocean wave simulation and prediction in our research project separately.

1.2.1 Marine Mesh Network

Thanks to the extensive cellular and WiFi wireless network coverage on land, broadband connectivity at anytime and anywhere has been taken for granted in many aspects of our daily lives and industrial operations. However, the wireless communication scenes change dramatically when one moves just several miles away from the coast into the sea. Cellular coverage starts to fade away. WiFi signals are non-existence. Ships, oil-rigs, ocean sensors, and all the industry and people that work around them are in critical need for other alternatives to maintain broadband connectivity with the rest of the world [Rea], which are essential for the safe, flexible, manageable and efficient functioning of these ocean entities and the quality of lives of the people working in the sea.

Unfortunately, none of the current marine communication technologies can provide broadband services that can satisfy such user needs. Existing wireless technologies used in ocean can be categorized into four types. The first type is satellite communications. Available anywhere in the world, satellite communications can provide wireless services to both static and mobile vessels.

However, satellite services are expensive and only provide very limited bandwidth. A typical satellite service can charge over $1000 per month for 1000 MB of data [Sat], which is not necessarily affordable for many individuals and small businesses. In addition, satellite communications have long delay in data transmission. The second option is MF, HF, or VHF radios for ship to shore communications. These technologies are narrow band and can only support voice communications due to the lack of bandwidth. The third type is undersea fiber, which can be used to wire remote ocean site to the shore. The cost of deploying the fiber, however, is extremely high (i.e. roughly $100k per km). Finally, point-to-point land-based microwave, where point-to-point wireless links are maintained among a land unit and an ocean unit, can also be used to connect static marine platforms to shore. This technology provides lower-cost and higher-capacity communications than satellite. However, line-of-sight microwave service can only reach about 30 km off the shore, limiting the service range significantly. In summary, all the existing techniques are either too expensive with very small bandwidth, or too limited in its coverage range, or both.

We propose to develop a marine wireless mesh network that is formed by low cost buoyed wireless base stations, as shown in Figure 1.1. A floating wireless base station with its anchor can be simply dropped into the water. Once in the water, these base stations start to harvest energy from ocean waves and self-organize into a mesh network. Each base station is equipped with a novel and extremely efficient energy harvesting unit that can continuously generate 50~100 watts of energy in typical sea states. With such high energy supply, a single base station can easily provide omni-directional wireless coverage of tens of kilometers range. With the help of multihop relaying, a mesh network formed by these self-powered base stations can provide wireless broadband coverage for more than 100 km off shore, which is enough to satisfy the vast majority of the communication needs for ships and oil platforms in ocean.

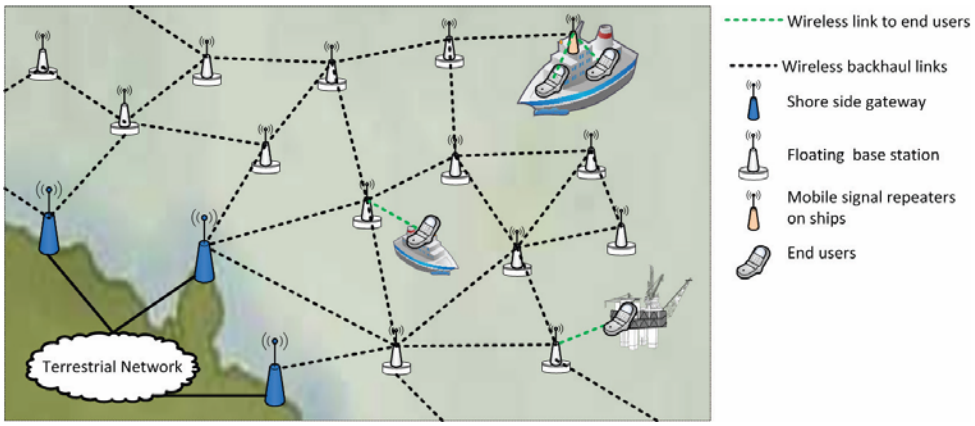

Figure 1.1 Illustration of a Marine Mesh Network

1.2.2 Role of Ocean Wave Simulation in MMN

In the MMN, the antenna of base station is mounted on buoy. Due to the stability of buoy, the antenna is neither suitable nor able to be mounted too high. Usually, the height of antenna can only reach 4-5 m, so the line of sight between two buoys is often blocked by ocean waves, as shown in Figure 1.2. Assume the antenna height is 3 m and the wave height (from crest to trough) is 6 m, both buoys are in the trough and move toward the crest simultaneously, then there will be about 50% of the time that the link cannot be established. If we use a general network protocol, the two nodes can only continuously try to communicate, which is not only energy-consuming, but also useless. Therefore, we need to design a network protocol that can sense and predict the height of buoys and only send data when the node find that its height is sufficient for communication.

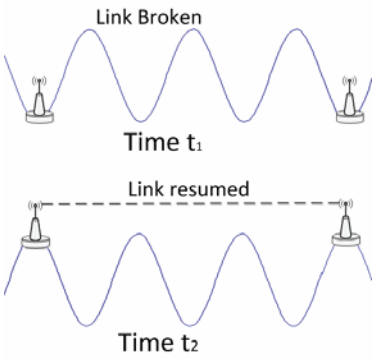

Figure 1.2 Link State versus Wave State

Before designing such a wave-state-aware network protocol, we need to know what oscillation characteristics ocean waves have and how they affect the communication between nodes. Therefore, we must be able to simulate the movement of ocean waves to obtain the height of some points on the sea surface, and then calculate whether there is a line of sight between two different points. After the protocol is designed, we also need to use this simulation software to verify the validity of the protocol. Therefore, ocean wave simulation is an indispensable test platform in protocol design process.

1.2.3 Role of Ocean Wave Prediction in MMN

Simply sensing the height of node can only save unnecessary energy consumption, but cannot improve network throughput. In order to improve network throughput between two locations, we adopt a cluster-based network structure, as shown in Figure 1.3. When two locations which are far apart (e.g. 10 km) want to communicate, we can place multiple buoys at each location to form two clusters. Nodes within a cluster possess the same data but have different instantaneous height (because their horizontal coordinates are different). When the number of buoys in a cluster increases, there will be a greater probability to ensure that at least one buoy in this cluster is high enough to be used to send data, so the continuity of communication between two clusters can be maintained. As a result, the network throughput is increased, and the degree of communication limitation between two locations is greatly reduced.

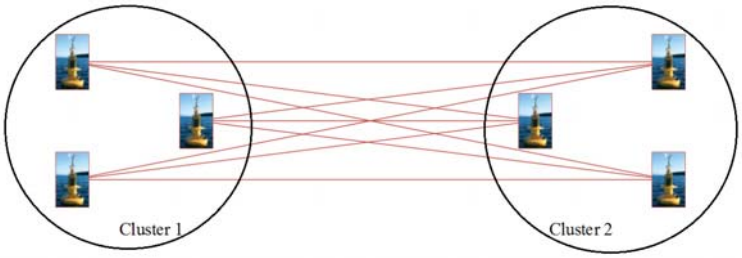

Figure 1.3 Cluster-based Network Structure

When two clusters want to communicate with each other, they have to select the highest node in each cluster to be responsible for communication. However, the height of a node is constantly changing, the highest node may sink in the future and other nodes may become the new highest node. At this point, we have to transfer the communication task to the new highest node. In order to know which node will become the new highest node, we must be able to predict the motion trend of each node, which is the purpose of our prediction.

1.3 Contribution

This thesis mainly designs and implements two methods of ocean wave prediction and a method of ocean wave simulation. The main contributions are as follows:

(1) An oscillation measurement method that can be applied in marine environment is designed and implemented. Traditional oscillation measurement methods usually need additional mechanical structures or expensive optical devices so that they are not suitable for marine environment. We propose an oscillation measurement method based on accelerometer. This method can realize real time measurement of wave height by relying only on on-chip accelerometer. Experiment results show that this method has an excellent accuracy.

(2) Aiming at nonlinear waves, an ocean wave prediction method based on Elman neural network is proposed. The neural network can learn and predict the oscillation mode of ocean wave. By comparing the effects of various neural networks, we finally select Elman neural network to conduct the prediction. The learning and prediction process of neural network is designed and implemented. Experiment results show that Elman network has an excellent accuracy in ocean wave prediction.

(3) Aiming at linear waves, an ocean wave prediction method based on multiple linear regression is designed and implemented. Although the neural network can predict ocean wave, it takes a long time (e.g. a few minutes) for training and prediction. We design and implement a multiple linear regression method which can predict ocean wave in real time. Experiment results show that the proposed method is superior to all kinds of neural networks in real time performance, and its prediction accuracy for linear waves is even higher than that of other neural network methods.

(4) An ocean wave simulation method is implemented and improved. This method is proposed by Tessendorf [Tes01], but there are some problems in the process of implementation, such as a) there are some fixed points in the animation of ocean wave. The height of these points do not change with the fluctuation of sea surface, thus, they affect the reality of simulation. By modifying the program, we eliminated the harmful effects of fixed points. b) The method proposed by Tessendorf mainly pursues visual effects, but the change of wave height with wind speed is not consistent with real marine environment. This thesis proposes a modification method that makes it consist with the real marine environment, so that improves the reality of simulation.

1.4 Thesis Organization

The rest part of this thesis are organized as follows:

(1) In chapter 2, we introduce the research status of ocean wave simulation and prediction and compare the advantages and disadvantages of various methods.

(2) In chapter 3, we propose a method for measuring ocean wave oscillation and show the experiment results.

(3) In chapter 4, we design and implement an ocean wave prediction method based on Elman neural network for nonlinear waves and show the experiment results.

(4) In chapter 5, we design and implement an ocean wave prediction method based on multiple linear regression for linear wave and show the experiment results.

(5) In chapter 6, we introduce the mathematical principle and implementation process of the ocean wave simulation in detail.

(6) In chapter 7, we conclude the thesis.

Chapter 2 Related Work

In this chapter, we introduce the research status of ocean wave simulation and prediction separately and compare their advantages and disadvantages.

2.1 Method of Ocean Wave Simulation

At present, the method of ocean wave simulation can be mainly classified into three types, which are based on physical model, geometric model and spectral model respectively.

2.1.1 Physical Model

Physical model uses classical hydrodynamics to describe wave motion. The motion of water particles is represented by fluid dynamic equations (e.g. Navier-Stokes equation). This method is perfectly realistic and can physically represent dynamics of all types of fluid, but the computation of Navier-Stokes equation is complex and the frame rate is low.

Some scholars have ever tried to simplify it. Kass et al. [Kas90] uses simplified numerical methods to solve the Navier-Stokes equations for animation of water waves. Thurey et al. [Thu07] proposed a simplification of the Navier-Stokes equations to offer real-time simulation of shallow water under some restrictions.

However, when simulating a large scene, it is still too time-consuming and cannot display real time animation.

2.1.2 Geometric Model

Geometric model mainly describes the particle motion of ocean surface, it represents the ocean surface as a sum of periodic functions (e.g. trigonometric function).

The first theory to describe ocean surface in terms of motion of individual points is proposed by physicist Gerstner in 1802. He showed that the motion of each water particle is a circle of radius r around a fixed point, therefore, a wave profile can be described by a mathematical function called trochoid [Fou86]. The first description of water waves in computer graphics was presented

by Fournier et al. [Fou86]. They simulated a train of trochoids by using a mix of Gerstner and Biesel swell models and solved the problems of propagation direction and phases. In the same year, Peachey et al. [Pea86] proposed the generation of height field by computing the superposition of several long-crested waveforms. They used particle systems to model the foam produced by wave breaking or colliding with obstacles [Pui14]. Ts'o et al. [Ts'o87] proposed a more precise way to solve the propagation problem by approximating the resulting ocean surface with a Beta-spline surface [Pui14]. Later, Gonzato et al. [Gon00] proposed a complete geometrical model accounting for refraction, diffraction, reflection, transmission and multiwave trains.

This kind of method is simple, low requirement for hardware and can be conducted in real-time, but the generated scenes are less realistic. It is often used in scenario which has low requirement for fidelity.

2.1.3 Spectral Model

Spectral Model approximates the state of the sea by using wave spectrum. It assumes that the sea state can be considered as a combination or superposition of a large number of regular sinusoidal wave components with different frequencies, amplitudes, and directions [Pui14]. After acquiring wave spectrum, it uses Fast Fourier Transform (FFT) to transform wave spectrum to the corresponding ocean wave.

As an example of these oceanographic measures, in 1964, Pierson et al. [Pie64] developed a model for the spectrum of fully developed wind seas on 460 ship-recorded waves [Pui14]. Spectral solutions were firstly introduced to computer graphics by Mastin et al. [Mas87] in 1987. The basic idea is to produce a height field having the same spectrum as the ocean surface. Later, Premoze et al. [Pre00] combined physical models and spectral models, but the obtained solution was only adequate for calm sea. Tessendorf [Tes01] explained simulating ocean water based on FFT in detail, his results has been used for the special effects of many movies such as Waterworld or Titanic. More recently, Mitchell [Mit05] introduced a Fourier-based GPU-synthesized height and normal maps. Gonzato et al. [Gon08] proposed a semiautomatic method to reconstruct the surface of the ocean from a video containing a real ocean scene. Nielsen et al.

[Nie13] proposed a method to allow artists to quickly sketch the wave's appearance and automatically approximate and animate them [Pui14].

This kind of method is highly realistic, but it needs complex mathematic model and massive computation (but less than physical model). In conclusion, it is adequate for real-time rendering.

Consider the characteristics of these three ocean wave simulation methods and our demands, it is not difficult to find that the spectrum-based ocean wave simulation method is the most suitable method for our scenario. It can guarantee a certain degree of reality and ensure that the computational complexity is not too high. Therefore, this thesis uses the spectrum-based method to simulate ocean waves and provides a test platform for the design of our MMN.

2.2 Method of Ocean Wave Prediction

According to different marine environments, ocean waves can be categorized into linear waves and nonlinear waves. If the wind speed of a sea area is low and steady for a long time, the ocean waves will also present relatively steady characteristics, such as relatively steady wavelength, amplitude, and period. In this case, the ocean waves belong to linear waves. Linear waves usually appear in deep water areas and climate-friendly areas. If the weather of an area is bad and changes rapidly, the movement of ocean waves will also be violent and its rhythmicity is not obvious, in this case, the ocean waves belong to nonlinear waves. Nonlinear waves usually appear in shallow water areas or bad weather areas. Take near-shore waves for example, due to the influence of changing of submarine topography, the wave frequency and wave height will increase gradually, and the wave will break on the shore finally. This kind of waves do not have steady characteristics, thus belong to nonlinear waves.

The prediction method of ocean waves can also be categorized into linear waves' prediction and nonlinear waves' prediction. The prediction methods for linear waves mainly include time series model, Kalman filter, etc. The prediction methods for nonlinear waves mainly include support vector machine, neural network, etc.

2.2.1 Prediction Method for Linear Wave

Literature [Pen06] [Lin11] [Lu14] [Wan15] [Ge16] proposed a kind of ship motion prediction method based on time series analysis, which usually use models like AR (Autoregressive), MA (Moving Average), ARMA (Autoregressive Moving Average), etc. This kind of method can use historical data of ship motion to model and predict, it doesn't have to know the state equation of ship motion. The advantages of this method is simple and has a good real time performance. It also has good prediction accuracy for linear systems. However, under severe sea state, the motion of ocean waves is nonlinear and random, in this case, the prediction results of this method often fail to meet the requirements.

Literature [Tri81] [Tri82] [Tri83] [Kuc11] [Rad13] [Pen15] proposed a kind of ship motion prediction method based on Kalman filter. The Kalman filter works in a two-step process. In the prediction step, it produces estimates of the current state variables, along with their uncertainties. Once the outcome of the next measurement is observed, these estimates are updated using a weighted average, with more weight being given to estimates with higher certainty [Kal]. This kind of method is first used in the field of ship motion prediction by M. S. Triantafyllou, M. Bodson, and M. Athans at the MIT. They use the basic principles of mechanics to analyse the force of a ship at sea, derive the ship motion state equation, and then use Kalman filter to predict the ship's motion. This kind of method has advantages of small amount of calculation, good real time performance, and ability to filter out measurement noise, but the prediction accuracy and stability are poor. This is because it needs to obtain the accurate state equation of ship motion, but in real environment, the ocean wave motion may be nonlinear and time-varying, so it is difficult to obtain a state equation suitable for different sea states. Therefore, this method cannot be directly applied to real marine environment.

2.2.2 Prediction Method for Nonlinear Wave

Literature [Zho10] [Fu10] [Luo14] [Yan15] [Luo16] proposed a kind of ship motion prediction methods based on support vector machine. This method maps the sample data from low-dimensional nonlinear space to high-dimensional linear space through kernel function, and then solves a linear function in high-dimensional space that can accurately indicate the relationship

between output data and input data. This method has the advantages of less training samples, avoiding local optimal solutions and strong generalization ability, but also has problems such as long training time, high computational complexity of the training process, in addition, the prediction accuracy is affected by kernel function.

Literature [Ge17] [Fu15] [Li16] [Pen17] [Mas11] [Zha14] proposed a kind of ship motion prediction method based on neural networks. This method uses historical data of ship motion to train neural networks. Through training, the neural network can automatically find the mapping relationship between input and output, which can avoid the process of data analysis and ship modeling. The advantage of this method is that it has strong data fitting ability and high accuracy. The disadvantage is that the computational complexity is high and the parameter selection is difficult.

2.2.3 Comparison of Prediction Method

Table 2.1 compares the advantages and disadvantages of several common prediction methods. Overall, linear methods have lower computational complexity but poor generalization capabilities. The nonlinear methods have higher computational complexity, but the generalization capabilities are good.

Table 2.1 Comparison of Prediction Methods

Prediction Method	Advantages	Disadvantages
Time Series Model	● Low computational complexity [Pen17] ● Easy to implement [Fro10]	● Not suitable for nonlinear problems ● Difficult in dealing with noisy data [Kha16] ● Poor prediction quality [Wan15] ● Lacks long-term prediction capability [Yan08], [Fro10], [Lu14], [Wan15]
Kalman Filter	● Intuitive, engineering way of	● No generalization capability

	constructing approximations [Per10] ● Computationally efficient ● Theoretical stability available ● Process noise data effectively [Lin11]	● Does not work in considerable nonlinearities ● Difficult to achieve online prediction [Lu14] ● Requires equation of motion which is difficult to obtain [Tri83], [Lu14] ● Not accurate in long-term (e.g. exceed 5s) prediction [Kha16]
Support Vector Machine	● Good generalization capability [Luo16] ● Less over fitting and robust to noise [Min05], [Msi07] ● No local minimal	● Computationally expensive in training [Msi07], [Aur08] ● Lack of transparency of results ● Selection of kernel function
Neural Network	● Strong in generalization ability [Mul12] ● Suitable for problems which are difficult to specify mathematically ● Efficient for online learning	● Slow training speed ● Need a large number of training samples ● Limited ability to explicitly identify possible causal relationships [Mul12] ● Prone to over fitting

In this thesis, we proposed ocean wave prediction methods for linear waves and nonlinear waves respectively, in which multiple linear regression method is used for linear waves, Elman neural network method is used for nonlinear waves.

The prediction accuracy of multiple linear regression is similar to that of time series model and Kalman filter, but it has faster calculation speed and simple principle. It does not need to establish mathematical model or motion state equation.

The prediction accuracy of Elman neural network is higher than other neural network methods. This is because most neural networks that used for ocean wave prediction are feed-forward

neural networks. The feed-forward neural networks belong to a static neural network and is not suitable for dynamic environments such as marine environments. The Elman neural network belongs to recurrent neural network and has a feedback loop. Thus, it has a good adaptability to uncertainty caused by external disturbance, system parameter variation and nonlinear characteristics. Therefore, its dynamic response performance is obviously superior to the feed-forward network.

Chapter 3 An Accelerometer based Wave Measurement Method

In order to design a wave-state-aware networking protocol, we must be able to sense the wave height. In this chapter, we propose a method to measure the real time wave height. Experiment results show that the method has a high accuracy. Section 3.1 to Section 3.3 describe the basic principles, implementation process and experiment evaluation of wave height measurement respectively.

3.1 Basic Principles

The measurement methods of oscillation can be divided into three types: mechanical measurement method, optical measurement method and electrical measurement method. Measuring the motion state of a buoy by using the integrated sensor in the main board is a kind of electrical measurement method, which is an inexpensive and feasible method. Neither does it require to install additional mechanical structures around the buoy, nor does it require to use expensive laser rangefinders. Thus, it becomes our first choice for wave height measurement.

Since the acceleration sensor integrated in the main board can only measure acceleration instead of displacement, we have to calculate the integral of acceleration to obtain speed, and then calculate the integral of speed to obtain displacement. Due to the error of accelerometer, during these two integrations, the error will be accumulated and amplified, result in the drift of final result. Figure 3.1 shows the result of directly integrating the acceleration.

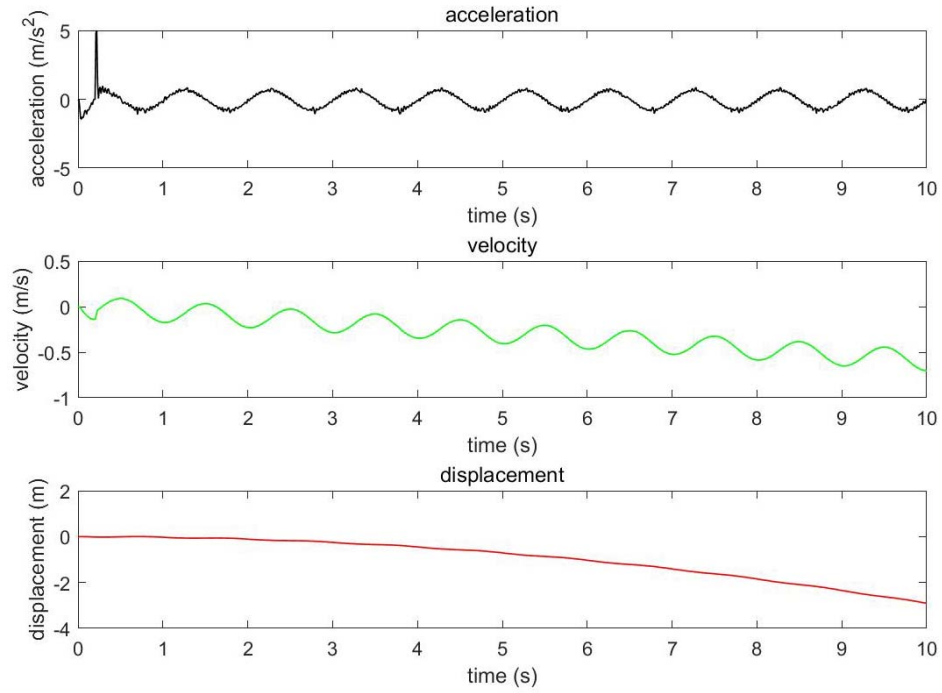

Figure 3.1 Results of Integration

In this experiment, we used an oscillation generator to generate a sine wave with amplitude of 1.9 cm, but due to the error of accelerometer, the results of velocity and displacement drifted after integration. The error of displacement has completely covered the original oscillation, so that the oscillation cannot be seen from the displacement figure. Within 10s, the displacement has drifted by 3 m, which is more than 150 times of the original amplitude. If the experiment continues, the drift of displacement will continue to increase. Therefore, how to eliminate the drift of displacement has become an urgent problem to be solved.

3.2 Implementation Process

Since the drift of displacement is not a strict polynomial function, it is difficult to eliminate it by using formula “displacement curve - drift curve”. Due to the frequency of drift is relatively low (0-0.1 Hz) but the frequency of original oscillation is relatively high (1 Hz), we consider to use filter to eliminate the drift. The filtering method is mainly divided into three steps. The first step is to obtain the spectrum of acceleration, velocity and displacement; the second step is to design

filter according to the spectrum; the third step is to filter the displacement data to get original oscillation data.

Figure 3.2 shows the spectrums of acceleration, velocity and displacement. Since the oscillation frequency generated by the oscillation generator is 1 Hz, the acceleration spectrum has a peak at the position of 1 Hz. However, after integrating the acceleration into velocity, we found a higher peak in the low frequency part (0-0.1 Hz) and its height has far exceeded the height of 1 Hz peak. This higher peak is just the accumulated error caused by integral. Similarly, after integrating the velocity into displacement, we found that the high peak in low frequency part (0-0.1 Hz) increased again, and the peak at 1 Hz is completely invisible. It indicates that the drift has completely overwhelmed the original oscillation. It can also be confirmed in Figure 3.1 that the displacement figure is unable to tell any oscillation characteristics, but only shows a downward trend in the macro level.

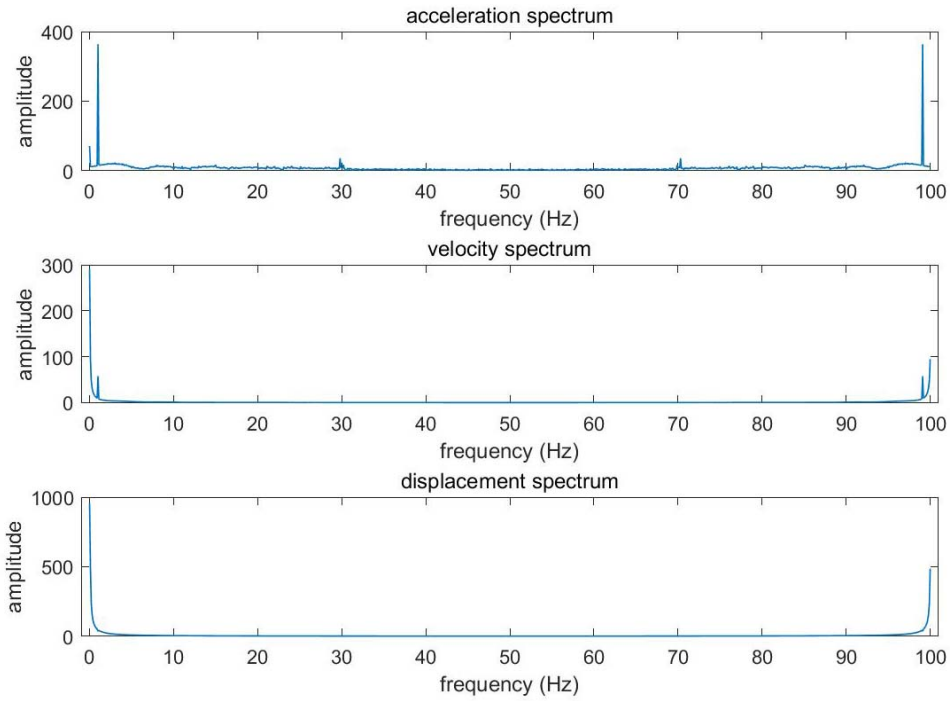

Figure 3.2 Spectrums of Acceleration, Velocity and Displacement

Therefore, we need to use a high-pass filter to retain the high-frequency part (1 Hz) and filter the low-frequency part (0-0.1 Hz). In order to ensure that the part near 1 Hz can be completely retained, we can set the cutoff frequency as 0.5 Hz, in which the cutoff frequency refers to that

the energy of wave in this frequency will be reduced to half. Figure 3.3 shows an example of a filter. The unit of x-axis is $\times \pi$ *rad* / *sample*, the relationship between Normalized Frequency and Hertz is as follows:

Suppose we want to find the value of Normalized Frequency corresponding to *x* Hz, then we can use the equation (3.1) to calculate

$$Normalized\ Frequency = 2x / fs \tag{3.1}$$

in which *fs* is the sampling frequency and *fs*=100Hz in our thesis.

Therefore, the Normalized Frequency value corresponding to 1 Hz is 0.02. It can be seen from Figure 3.3, to the left of 0.02, the magnitude response curve of the filter is sharply declined, indicates that waves below 1 Hz will be filtered out.

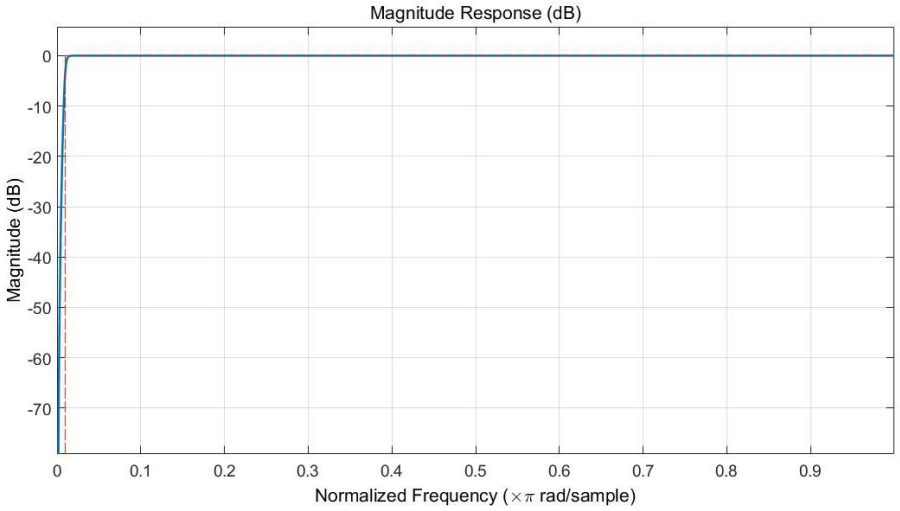

Figure 3.3 Magnitude Response Curve

3.3 Results and Analysis

Figure 3.4 shows the filtered results. It can be seen that after filtering, the displacement curve is highly consistent with the original oscillation curve. The average amplitude of the original oscillation is 18.13 mm, the average amplitude of the displacement curve is 18.49 mm. Thus the error is only 0.3 mm, which is far more accurate than what we expected.

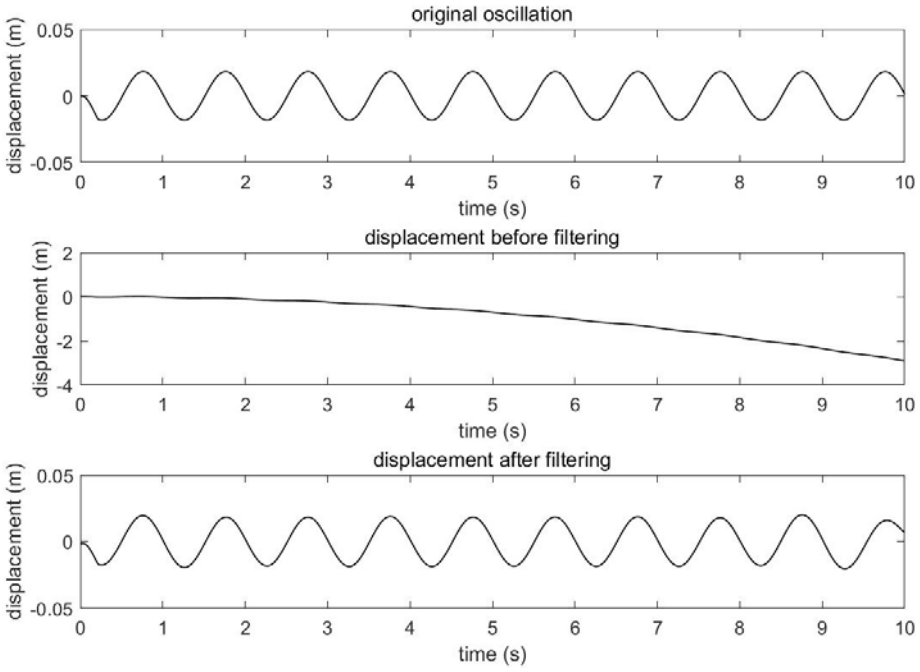

Figure 3.4 Filtered Results

Besides above laboratory experiment, we have also done a field experiment that put our accelerometer in a pond to measure the pond water oscillation. Figure 3.5 and 3.6 shows the results before filtering and after filtering respectively. It can be seen that before filtering, the displacement curve cannot reflect the oscillation characteristics of water waves, but after filtering, the displacement curve presents the same oscillation characteristics with acceleration curve, which means the filtered result is correct.

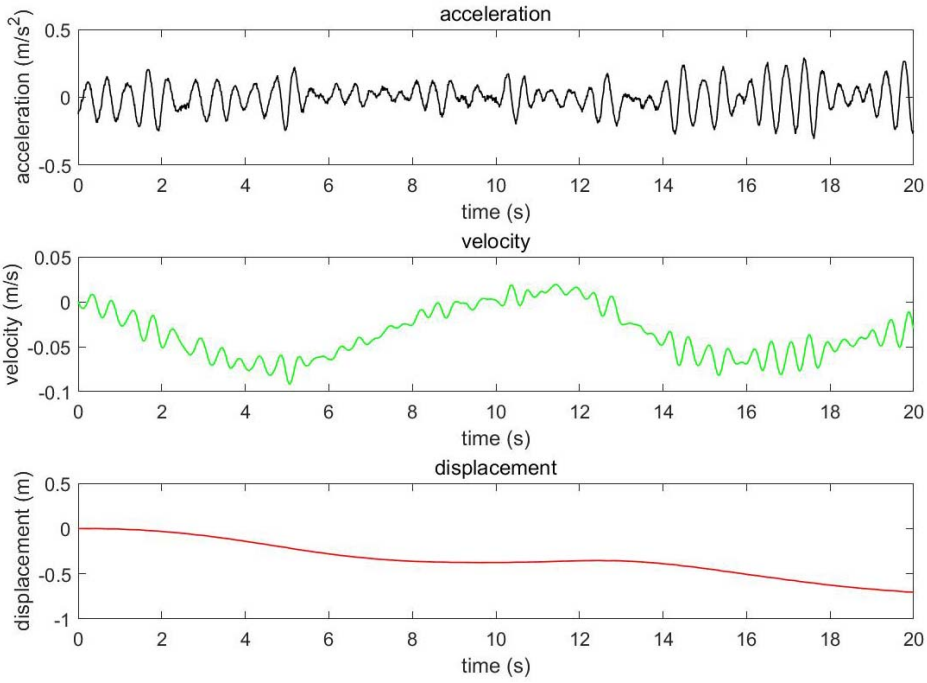

Figure 3.5 Results before Filtering

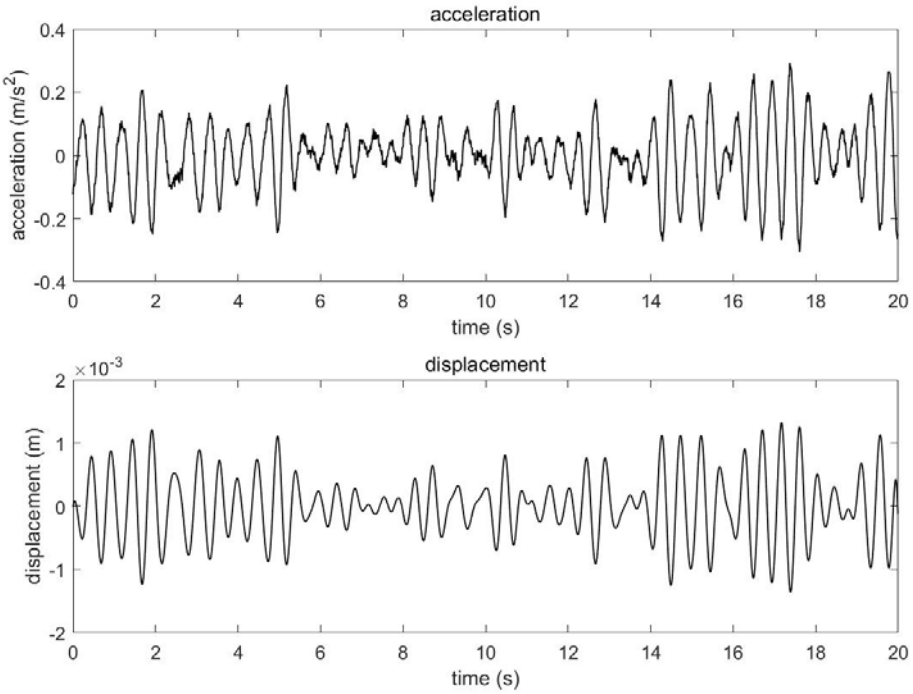

Figure 3.6 Results after Filtering

Chapter 4 A Neural Network based Ocean Wave Prediction Method

After we can measure the wave height, we need to use historical wave height data to predict future wave height. In this chapter, we propose a neural network based ocean wave prediction method for nonlinear waves, i.e. we can accurately predict the future height of a certain point on the sea surface. Section 4.1 introduces the motivation and theoretical basis of our ocean wave prediction. Section 4.2 introduces some related concepts of neural networks and a neural network (called Elman) which is suitable for ocean wave prediction. Section 4.3 introduces the implementation process of ocean wave prediction using Elman network. Section 4.4 shows and analyses the experiment results.

4.1 Motivation and Theoretical Basis of Ocean Wave Prediction

Since the MMN uses buoys to communicate, the height of a buoy (i.e. the height of ocean wave + the height of antenna) directly determines whether it can transmit and receive signals normally. Therefore, if the future height of a buoy can be predicted accurately, not only the success rate of communication can be significantly improved, but also the energy consumption can be significantly reduced.

Our prediction of wave height is based on the principle that ocean waves have the attribute of periodic oscillations. As shown in Figure 4.1, suppose we know that the average wave height of a certain sea area is 5 m and the oscillation period is 10 s. If we also know that the current height of a point (i.e. the black dot) is -2.023 m, and the point is in the process of rising, then we can figure out that the height of the point should be 0.7725m after 2 s (i.e. the blue triangle) and 2.5 m after 4 s (i.e. the red square). Of course, the above inference is based on the assumption that the oscillation waveform is a standard sinusoid, but the real oscillation waveform is not a standard sinusoid, so, there may be some errors in predicting results.

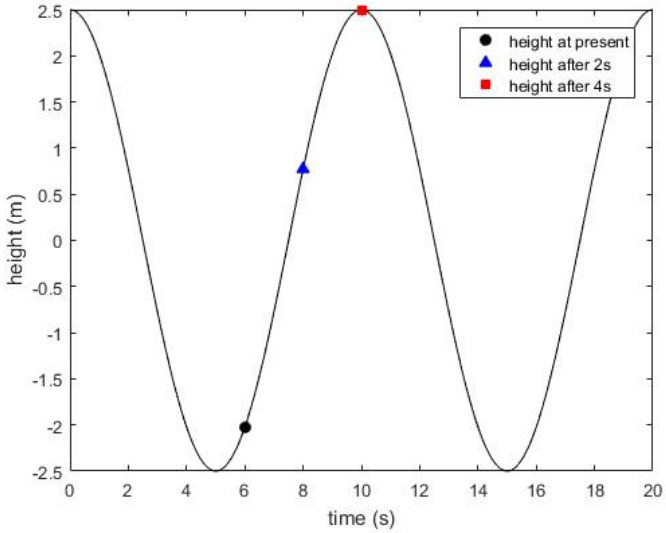

Figure 4.1 Theoretical Basis of Ocean Wave Prediction

To ensure the error will not be too large, the prediction process is performed in real time. We only use the wave height of current few seconds to predict the wave height of next few seconds, instead of using too old data (e.g. wave height data of a few minutes ago) to make predictions or try to predict the wave height of far future (e.g. a few minutes later).

4.2 Introduction to Neural Networks

In this section, we mainly introduce an Elman neural network which is suitable for ocean wave prediction. Subsection 4.2.1 introduces the related concepts of neural networks. Subsection 4.2.2 introduces the structure of Elman neural network and the reasons why we use it.

4.2.1 Related Concepts

Neural network is a kind of mathematical model that mimics the structure and function of biological brain to estimate or approximate a function. Figure 4.2 shows a typical neural network structure consisting of three layers of neurons. The output of each neuron is determined by the sum of its inputs. The connections between neurons have weights that can be constantly and automatically adjusted during the learning process so that the final output is close to the expected result gradually. Therefore, the training process of a neural network is the process of weights

adjustment. Finally, we will get a trained neural network model. When we input a new set of data, it can output a corresponding set of results.

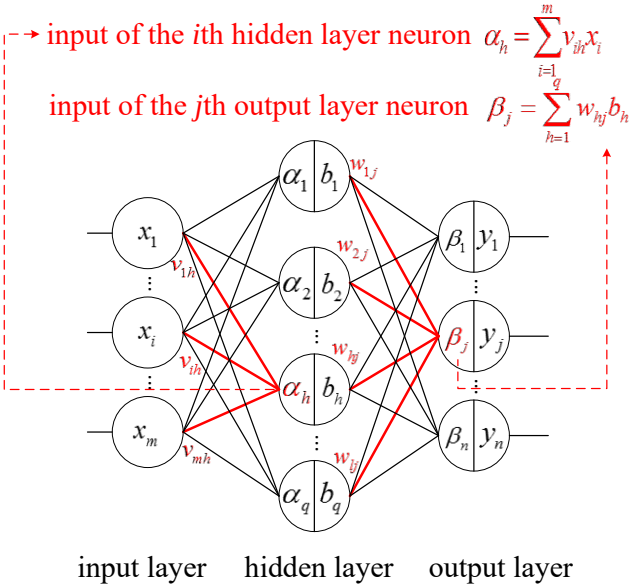

Figure 4.2 Typical Structure of Neural Network

In the previous subsection, we mentioned that given the current wave height and motion direction, we can figure out the future wave height, i.e., there is a relationship between current wave height and future wave height. Neural networks can learn this relationship. We take the current wave height as input and the future wave height as output. Using hundreds of such examples to train the neural network, so that the neural network will be able to learn the conversion relationship between them. After that, whenever we want to predict future wave height, we enter a set of current wave heights into the neural network, the neural network will return a set of future wave heights as results.

4.2.2 Elman Neural Network

Neural networks have a variety of structures, excitation functions and learning rules. This subsection focuses on a neural network called Elman. Elman networks (as shown in Figure 4.3) are feed-forward networks with the addition of layer recurrent connections with delays. It can learn any dynamic input-output relationship arbitrarily well, given enough neurons in the hidden

layers. The number of neurons in the input and output layers is determined by the problem to be solved. The number of hidden layer neurons needs to be artificially determined. It is generally considered that this number is related to the number of neurons in input and output layers or the complexity of the problem. However, there is no specific calculation formula, it should be determined by experiment.

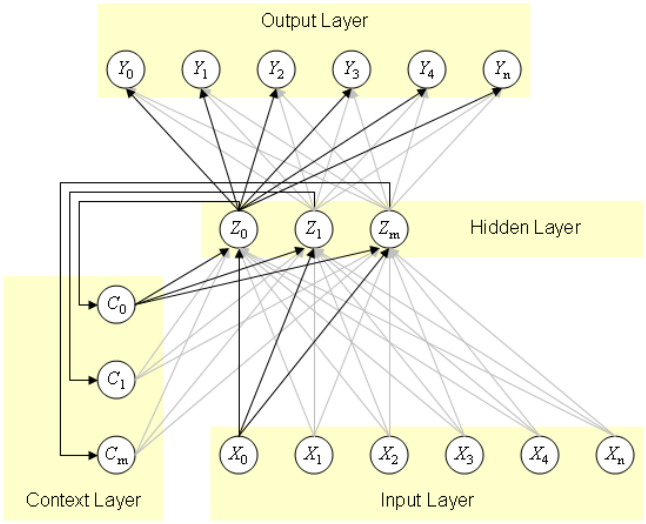

Figure 4.3 Structure of Elman Neural Network

It should be pointed out that it is not only the Elman network can achieve ocean wave prediction. We have tried more than ten neural network methods, the Elman network has a relatively good effect. Table 4.1 shows the various types of neural networks we have tried. The first eight methods are suitable for ocean wave prediction and are sorted according to their prediction effect. The latter six methods are not suitable for ocean wave prediction. They are not theoretically applicable because they were designed to solve classification problem originally, but our ocean wave prediction problem is regression problem. Their goals are different.

Table 4.1 Various Types of Neural Networks

Function Name	Function Description (and Application Fields)	Applicable
elmannet	Create an Elman back propagation network	Yes
newlind	Design a linear layer	Yes

newrb	Design a radial basis network	Yes
newrbe	Design an exact radial basis network	Yes
newgrnn	Design a generalized regression neural network	Yes
newff	Create a feed-forward back propagation network	Yes
cascadeforwardnet	Create a trainable cascade-forward back propagation network	Yes
newfftd	Create a feed-forward input-delay back propagation network	Yes
newp	Create a perceptron to solve linearly separable classification problems	No
newpnn	Design a probabilistic neural network to solve classification problems	No
newc	Create a competitive layer to solve classification problems	No
newsom	Create a self-organizing map to solve classification problems	No
newhop	Create a Hopfield recurrent network to solve pattern recall problems	No
newlvq	Create a learning vector quantization network to solve classification problems	No

4.3 Implementation Process

4.3.1 Training Method of Elman Network

The training method of Elman network directly affects the accuracy of ocean wave prediction, so how to determine the format and quantity of training samples is a very important issue.

In section 4.1 and subsection 4.2.1, we mentioned that it is required to train the neural network with the current wave height as input and the future wave height as output. Thus, the construction method of training sample is as shown in Figure 4.4, in which the attributes correspond to input data, the label corresponds to output data, and H represents the height of a certain point at corresponding time. For example, if we want to predict the height of 5 s later, the time interval between attributes and label should be 5 s.

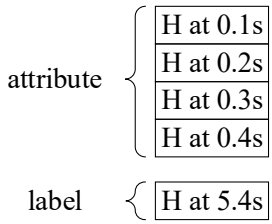

Figure 4.4 Structure of a Training Sample

We use hundreds of training samples like Figure 4.4 to form a training set, as shown in Figure 4.5, to train the neural network.

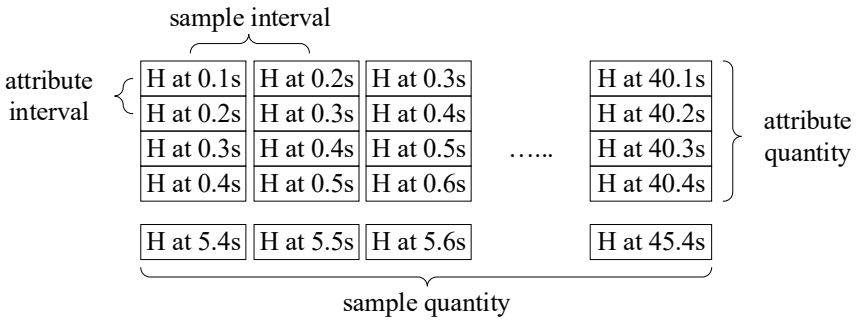

Figure 4.5 Structure of Training Set

One question that comes with it is how to determine the value of sample interval, sample quantity, attribute interval, and attribute quantity, because these four parameters will affect the training effect of the neural network.

Sample interval and sample quantity are a pair of related variables that determine the utilization of available training data. Under the premise that the available training data is constant, the larger the sample interval, the smaller the sample quantity. For example, we have 50 s of wave oscillation data that can be used to train the neural network. If we take a set of data every 1 s to form a training sample, we can compose 50 training samples; if we take a set of data every 0.1 s to form a training sample, then we can compose 500 training samples. In theory, the neural network trained by 500 samples should have a better prediction accuracy than the neural network trained by 50 samples. However, it doesn't mean the more the number of training samples, the better the prediction accuracy. When the quantity of training samples reach a certain number, the prediction accuracy of the neural network will no longer increase but even decrease. This is the

over-fitting phenomenon. In addition, the training of neural network takes a lot of time. If the sample interval is too small, the difference between two samples is also very small. Using these similar samples to train the neural network will not improve the prediction accuracy significantly.

Attribute interval and attribute quantity also affect the training effect of neural network. The reason why we want to set multiple attributes in a sample is to show the movement trend of a certain point in current period of time, which is helpful to judge the future height of this point. As shown in Figure 4.6, if we know that the point goes down firstly and then goes up in current period of time (4 s-6 s), which indicates that this point is currently in the wave trough, then it can be speculated that in the next 4 s, the point will rise to the wave crest. Conversely, if only one attribute is used, then we can only know the current height of the point, but we don't know whether the point is currently moving up or down, so we cannot speculate how high the point will be in the next few seconds. .

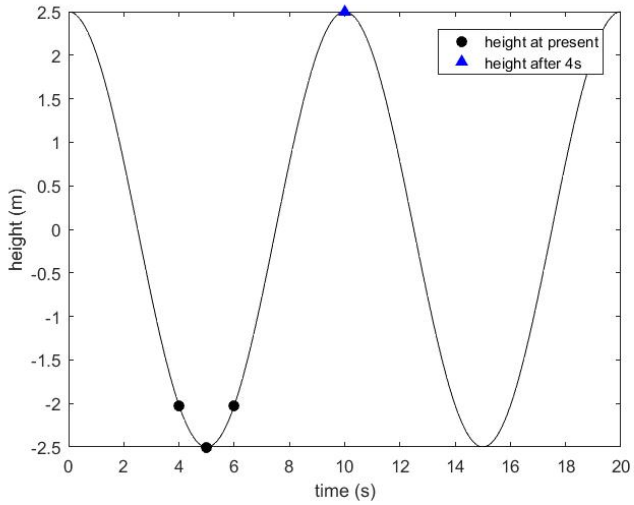

Figure 4.6 Oscillation Trend Analysis

Of course, it doesn’t mean the more the attribute quantity, the better the prediction accuracy. Too many attributes will affect the training speed of neural network, and it does not help to improve the prediction accuracy of neural network.

Similarly, the attribute interval should not be as large as possible, the key point is it should be able to describe the current motion state of the point. If the attribute interval is too large, it may not be able to describe the motion state very well. As shown in Figure 4.7, we measured that the

heights of a point in recent period (0 s-7.5 s) is 0, but we cannot know whether this point is moving up or down from this phenomenon. If the attribute interval is too small, misjudgment may occur. Because the oscillation of ocean wave is not a standard sine wave, it is a sine wave on macro level, but some jitter often appears on micro level. If the attribute interval is too small, these micro jitters will be mistakenly regard as the changing of oscillation direction, thus the current position of the point (e.g. on the wave crest or wave trough) will also be misjudged.

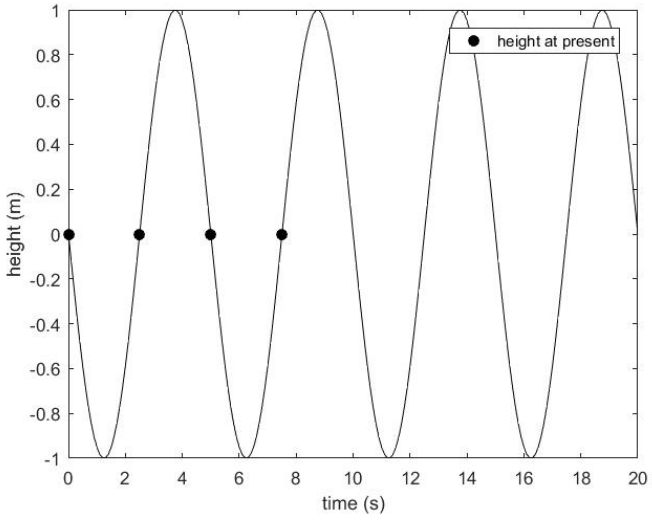

Figure 4.7 An Example of Invalid Attribute Interval

In addition to above four influence factors, the Elman network also has a parameter that needs to be artificially determined, that is, the number of hidden layer neurons. When the number is too small, the neural network is too simple to learn the complex relationships described by training samples, so the prediction accuracy is low. When the number is too large, the neural network will change from learning training samples to memorizing training samples and lose the generalization ability, i.e., it can memorize the samples very well, but for unlearned samples, its inferential capability is very low.

The setting method of this parameter is not clearly defined, the optimum value should be determined by experiment on a case by case basis.

4.3.2 Test Method of Elman Network

The test set of the Elman network should have the same format with the training set, as shown in Figure 4.8. That is, each sample in test set should have the same attribute quantity as that of training set, and the attribute interval should also be consistent with training set.

The only difference is that the test set does not contain labels, because the label is exactly what we want to get from experiment.

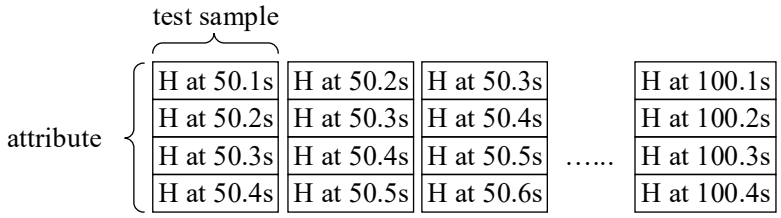

Figure 4.8 Structure of Test Set

4.4 Experiment and Results Analysis

In this section, we conduct two sets of experiments. One uses simulated ocean wave data, the other uses real ocean wave data. The simulated ocean wave data is generated by a simulator which is discussed in Chapter 6. The real ocean wave data is acquired by field measurement of marine institute. Subsection 4.4.1 introduces the experiment process and parameter setting. Subsection 4.4.1 shows and analyses the results.

4.4.1 Parameter Setting

4.4.1.1 Selection of Sample Quantity and Sample Interval

Subsection 4.3.1 mentions that the selection of these two parameters (i.e. sample quantity and sample interval) will affect the prediction accuracy of neural network. To find out the optimal value, we firstly set other parameters as shown in Table 4.2, and then test the prediction accuracy of the neural network with different sample quantity and sample interval.

Table 4.2 Parameter Setting to Test Optimal Sample Quantity and Sample Interval

Parameter	Value
Wind speed	20m/s
Attribute interval	0.5s
Attribute quantity	5
Prediction time span	5s
Test start time	1005s
Test end time	1105s

By testing the prediction accuracy with different sample quantity and sample interval, we obtained the results as shown in Figure 4.9. It can be found from Figure 4.9, when the sample interval increases, the prediction error has a tendency of decreasing, but after decreasing to a certain extent, it does not continue to decrease, but fluctuates within a certain range. Similarly, when the sample quantity increases, the prediction error also tends to decrease firstly, and then fluctuates within a certain range.

Results show that when the sample quantity is 400 and the sample interval is 0.5 s, the trained neural network has the best prediction accuracy. It should be pointed out that the measurement results of the optimal value are related to the parameters setting during the experiment, they are not unique determined value. When the experiment parameters (e.g. sea state) are changed, the optimal value should also be re-measured. The significance of this subsection is providing a test method to determine the optimal value, rather than providing a unique determined optimal value.

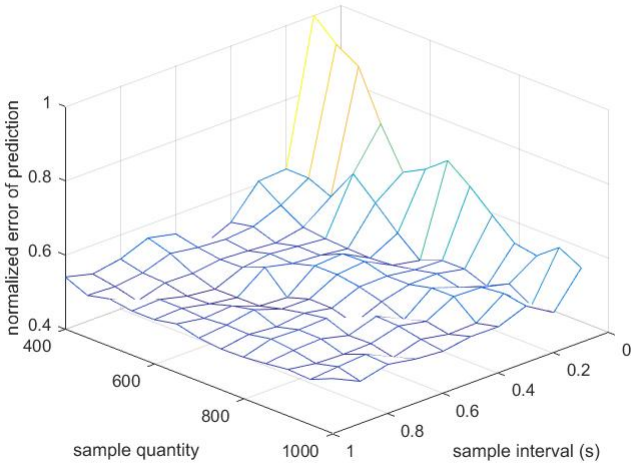

Figure 4.9 Prediction Error versus Sample Quantity and Sample Interval

4.4.1.2 Selection of Attribute Quantity and Attribute Interval

Similar to subsection 4.4.1, we tested the optimal value of attribute quantity and attribute interval by using the parameters shown in Table 4.3.

Table 4.3 Parameter Setting to Test Optimal Attribute Quantity and Attribute Interval

Parameter	Value
Wind speed	20m/s
Sample interval	0.5s
Sample quantity	400
Prediction time span	5s
Test start time	403s
Test end time	503s

By testing the prediction error with different attribute quantity and attribute interval, we get the results as shown in Figure 4.10. It can be found that as the attribute interval increases, the prediction error tends to decrease, but after decreasing to a certain extent, it does not continue to

decrease, but fluctuates within a certain range. Similarly, as the attribute quantity increases, the prediction error also tends to decrease firstly, and then fluctuates within a certain range.

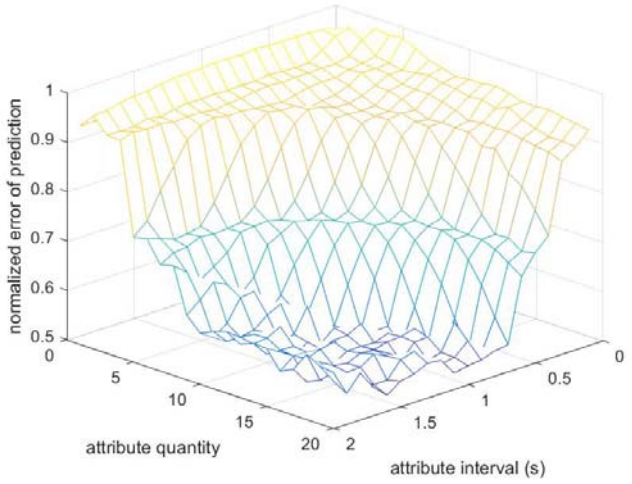

Figure 4.10 Prediction Error versus Attribute Quantity and Attribute Interval

The results show that when the attribute quantity is 17 and the attribute interval is 0.9s, the trained neural network has the best prediction accuracy. Similar to subsection 4.4.1, the significance of this subsection is also providing a test method to determine the optimal value, rather than providing a unique determined optimal value.

4.4.1.3 Selection of Number of Hidden Layer Neurons

The number of hidden layer neurons is usually related to the number of input and output layer neurons, but there is no exact setting method, it needs to be determined by experiment. Similar to subsection 4.4.1, we tested the number of hidden layer neurons with the parameters shown in Table 4.4. The results are shown in Figure 4.11.

Table 4.4 Parameter Setting to Test Optimal Value of Hidden Layer Neurons

Parameter	Value
Wind speed	20m/s
Sample interval	0.5s
Sample quantity	400

Attribute interval	0.9s
Attribute quantity	17
Prediction time span	5s
Test start time	395s
Test end time	495s

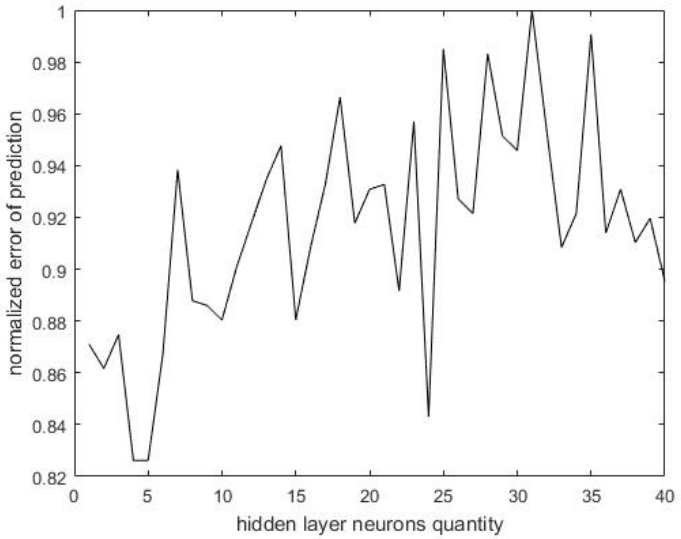

Figure 4.11 Prediction Error versus Number of Hidden Layer Neurons

Results show that when the number of hidden layer neurons is 4 or 5, the trained neural network has the best prediction accuracy. From Figure 4.11, it can be seen that there is no significant difference in prediction error when number of hidden neurons increases, thus we just need to select a relatively small number of hidden neurons to keep the neural network simple, because simple network means high calculation speed.

4.4.2 Results and Analysis

In this subsection, we show two kind of prediction results, one is based on simulated ocean waves, the other is based on real ocean waves.

4.4.2.1 Prediction Results for Simulated Ocean Wave

Figure 4.12 shows the prediction results of simulated ocean waves. The experiment parameters are the same as Table 4.4. It can be seen from Figure 4.12, the predicted value and the real value are highly consistent with each other except some slight differences in peak points.

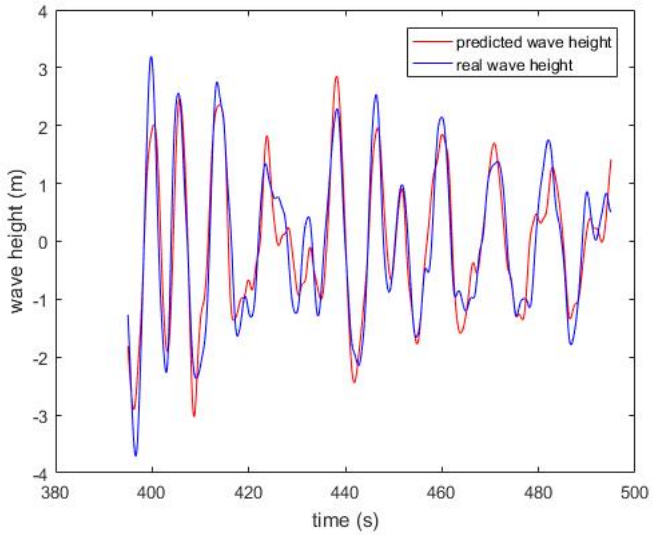

Figure 4.12 Prediction Results of the Elman Neural Network

Figure 4.13 shows the prediction accuracy of the Elman neural network. The x-axis is the target value and the y-axis is the predicted value. If data points are on the line y=x or close to this line, it indicates that the prediction is accurate. By fitting the data points, we can get the expression of the fitted line y=0.85x-0.0019, which is very close to the line y=x.

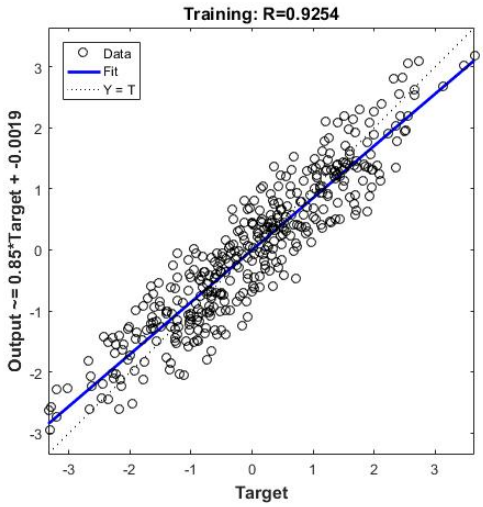

Figure 4.13 Prediction Accuracy of the Elman Neural Network

The R value in Figure 4.13 is the Pearson product-moment correlation coefficient, which is used to measure the correlation between two variables (e.g. predicted value and target value), and the value is between -1 and 1. Figure 4.14 shows the changing of R value with different distribution of two variables. The closer the R value is to 1 or -1, the stronger the linear correlation between two variables. In this case, R=0.9254, which indicates the method has high prediction accuracy.

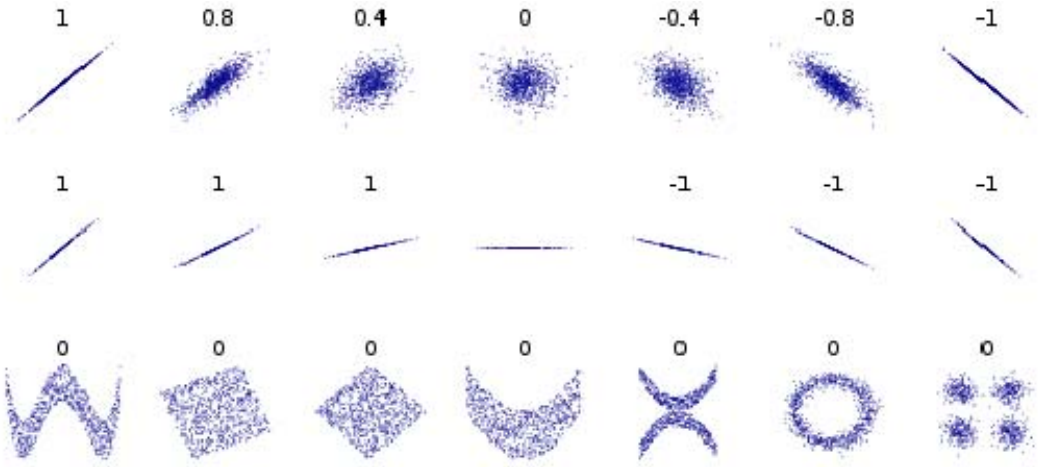

Figure 4.14 Distribution Characteristics of Different R Values

Figure 4.15 shows the prediction results whose time span is 1 s and 10 s separately. By comparison, it can be found that the prediction accuracy of short time span is significantly higher than that of long time span.

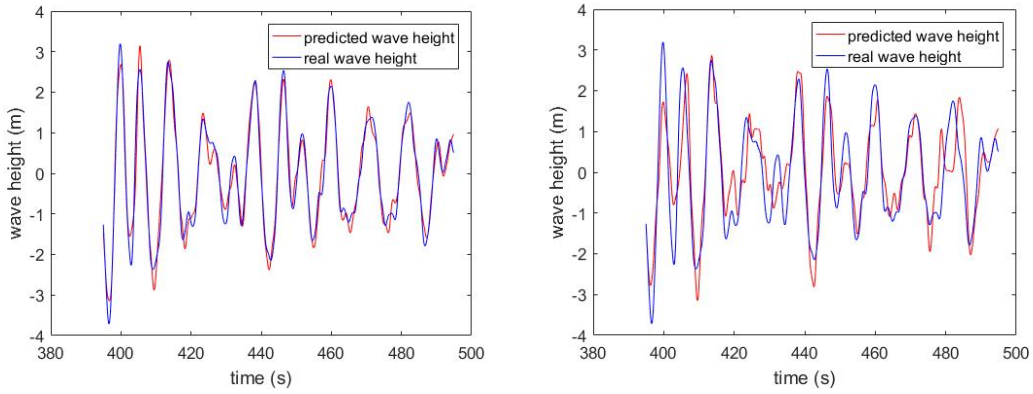

Figure 4.15 Prediction Results of Different Prediction Time Span

Figure 4.16 shows the prediction accuracy (i.e. R value) and the prediction error as a function of prediction time span. It can be found that as the prediction time span increases, the prediction accuracy shows a downward trend and the prediction error shows an upward trend. When time span is 0.5 s, the prediction error is approximately 1/5 of that when time span is 9 s.

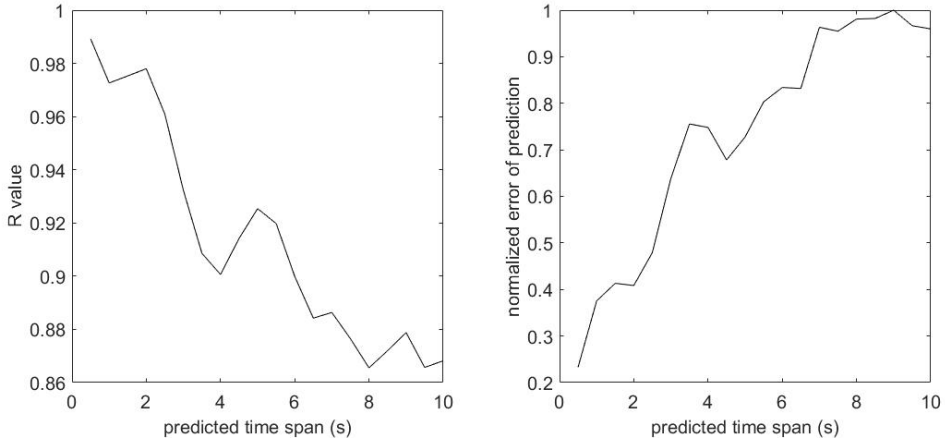

Figure 4.16 Prediction Accuracy of Different Prediction Time Span

To compare the performance differences between the Elman neural network and other kinds of neural networks in ocean wave prediction, we tested the first eight kinds of neural network methods in Table 4.1, the results are shown in Figure 4.17. The meaning of each line in Figure 4.17 is the same as the fitted line in Figure 4.13, which expresses the consistency between predicted values and real values. The black line is y=x, which means the predicted value is exactly match with the real value. If other lines are close to y=x, it indicates that their prediction accuracy is high. For example, the solid lines in Figure 4.17 are closer to y=x than the dashed lines, so the neural network methods corresponding to the solid lines have a higher prediction accuracy. However, judging the distance between two lines is very difficult, because except parallel lines, two lines will eventually have an intersection, and it is unable to define how the distance between two lines is calculated. Therefore, the indicator that is used to judge the prediction accuracy of neural networks is still the R value. Figure 4.17 sorts the R values of the eight neural networks from high to low. It can be seen that the Elman network has the best prediction accuracy. This is because the Elman neural network has feedback connections, which have a good adaptability to the uncertainty that caused by external interference, system parameter variation and nonlinear characteristics. So it is superior to the traditional feed-forward neural network in dynamic response.

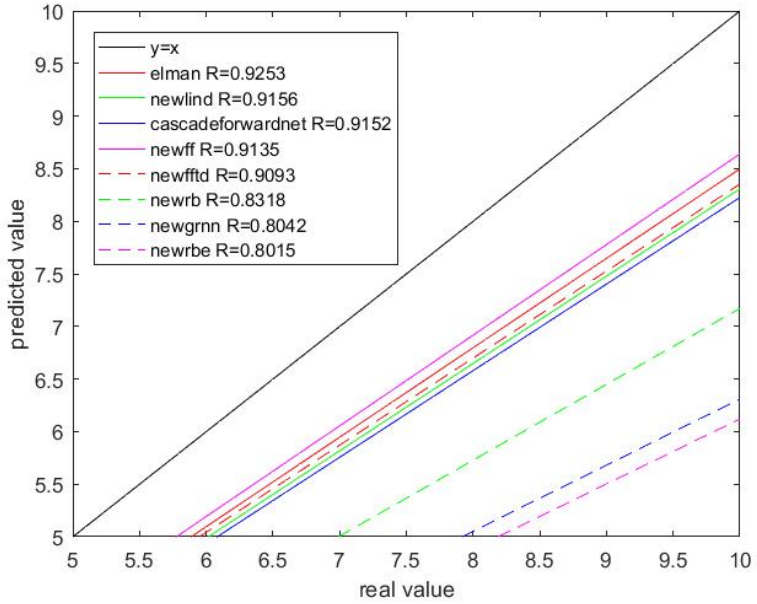

Figure 4.17 Performance Comparison of Various Neural Networks

4.4.2.2 Prediction Results for Real Ocean Wave

Besides simulation experiment, we also used real ocean wave data to test our prediction method. Figure 4.18 shows the real ocean wave data which is from literature [Ryc97] and originally supplied by M. Olagnon, IFREMER, France and P. Palo, US Naval Facilities Engineering Service Center.

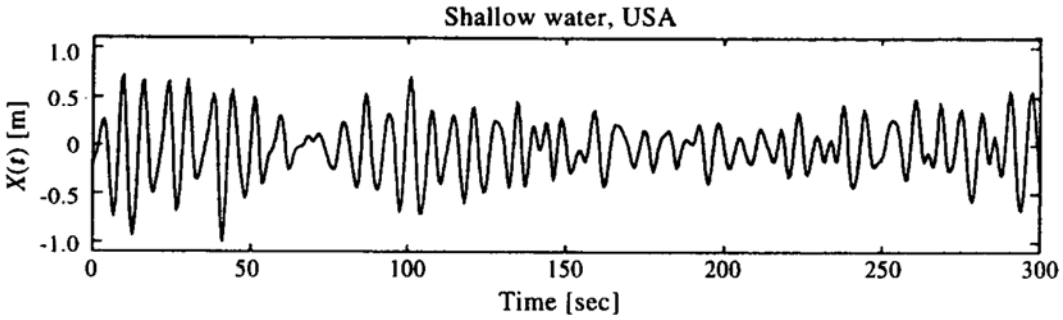

Figure 4.18 Real Ocean Wave Data

It is a kind of shallow water wave, which is more irregular than deep water wave. In other words, it is a kind of nonlinear wave. As mentioned above, neural network methods can not only predict

linear waves, but also predict nonlinear waves, thus, in this experiment, we test the prediction accuracy of neural network methods for nonlinear waves.

We use the first 200 s data to train the neural network and the last 100 s data to test the neural network. The parameter selection process is similar to Subsection 4.1.1 and need not to be repeated here. We just show the prediction results.

Figure 4.19 shows the prediction results of Elman neural network. Figure 4.20 shows the correlation coefficient comparison of various methods.

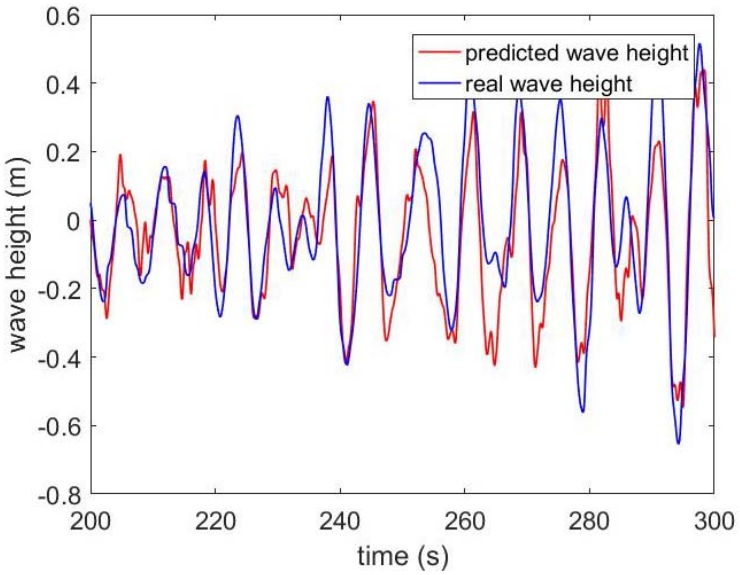

Figure 4.19 Prediction Results of the Elman Neural Network

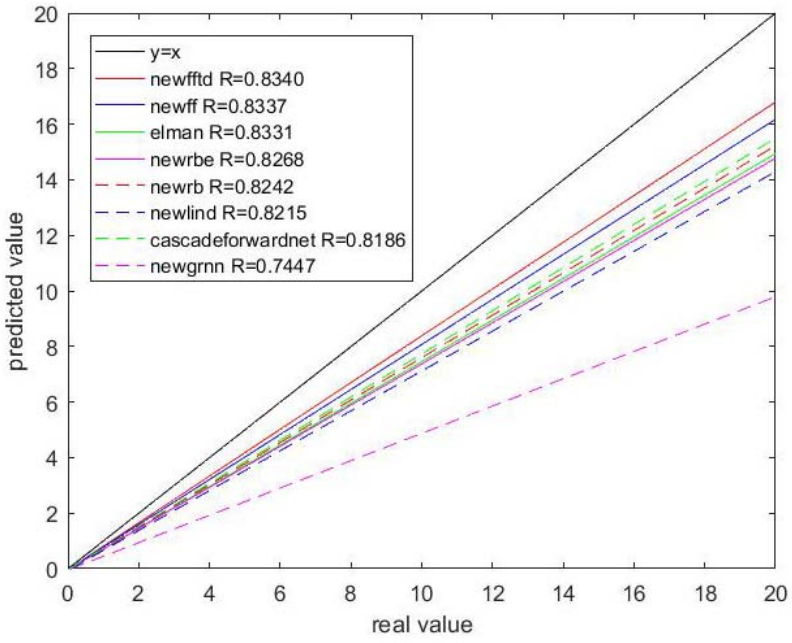

Figure 4.20 Correlation Coefficient Comparison of Various Methods

Figure 4.21 shows the comprehensive comparison of prediction error and R value. It can be seen that Elman method has the lowest prediction error and a relatively high R value. The computing method of prediction error is shown as follows:

$$\text{Prediction Error} = \text{Average}\ (\ |\text{Predicted Curve} - \text{Real Curve}|\ ) \tag{4.1}$$

For example, if the predicted curve is composed of 100 points (i.e. P(1), P(2), … , P(100)), the real curve is also composed of 100 points (i.e. R(1), R(2), … , R(100)), then the prediction error is:

$$\text{Prediction Error} = (\ |P(1)-R(1)| + |P(2)-R(2)| + \ldots + |P(100)-R(100)|\ ) / 100 \tag{4.2}$$

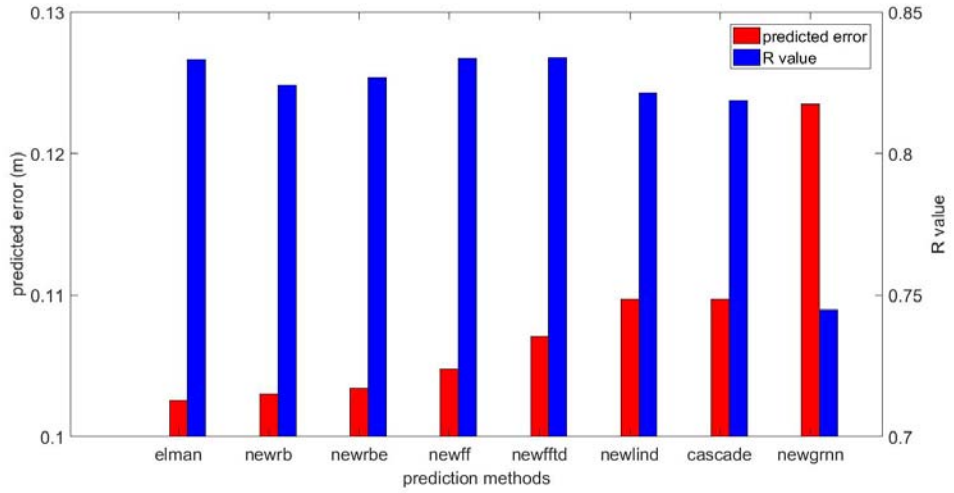

Figure 4.21 Comprehensive Comparison of Various Methods

Besides above laboratory experiments, we also did a field experiment, which uses the wave measurement method proposed in Chapter 3 to sense the water wave in a pond. Figure 4.22 shows the prediction results for pond water waves. It indicates that our Elman neural network method is not only effective in simulation, but also effective in real world.

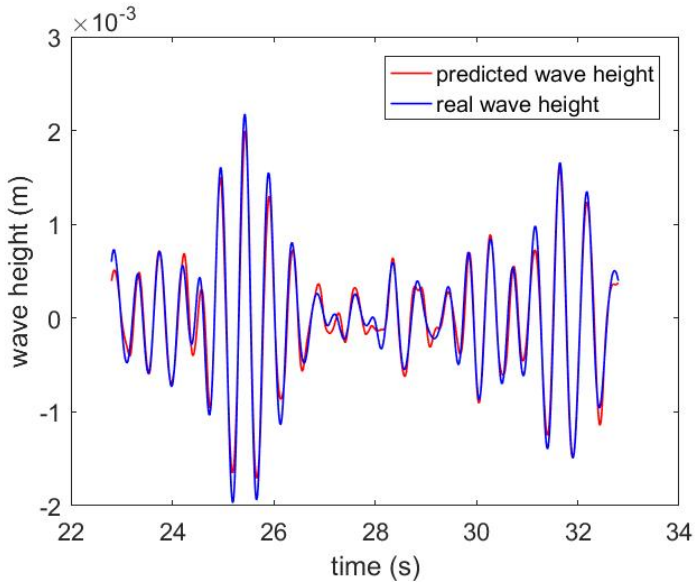

Figure 4.22 Prediction Results for Pond Water Wave

4.4.3 Conclusion

In this chapter, we conducted two sets of experiments. From the perspective of data sources, we tested our method with simulated data and real data respectively. From the perspective of wave types, we tested our method by linear waves and nonlinear waves respectively. Experiment Results show that our method can be used both in prediction of linear waves and nonlinear waves. In addition, through test with simulated data and real data, we demonstrate that out method is effective in real marine environment.

Compared with linear waves, nonlinear waves are more irregular, so the prediction accuracy of nonlinear waves is lower than that of linear waves. However, Elman network is still the best method in predicting these two kind of waves. Thus, this Chapter proposed an effective technology for our future networking protocol design.

Chapter 5 A Multiple Linear Regression based Ocean Wave Prediction Method

In this chapter, we implement an ocean wave prediction method based on multiple linear regression for linear waves. Section 5.1 introduces the basic principles of multiple linear regression. Section 5.2 introduces the theoretical basis for using multiple linear regression for ocean wave prediction. Section 5.3 introduces the specific implementation process of ocean wave prediction. Section 5.4 shows and analyses the experiment results.

5.1 Introduction to Multiple Linear Regression

In statistics, linear regression is a linear approach for modelling the relationship between a scalar dependent variable y and one or more explanatory variables (or independent variables) denoted X. The case of one explanatory variable is called simple linear regression. For more than one explanatory variable, the process is called multiple linear regression [Lin].

Given a sample $\mathbf{x} = (x_1; x_2; ...; x_d)$ described by d attributes, x_i is the value of $\mathbf{x}$ on the ith attribute, linear model attempts to learn a function that predict value through a linear combination of attributes, i.e.

$$f(\mathbf{x}) = w_1 x_1 + w_2 x_2 + ... + w_d x_d + b \tag{5.1}$$

Equation (5.1) can be generally written in vector form as

$$f(\mathbf{x}) = \mathbf{w}^T \mathbf{x} + b \tag{5.2}$$

in which $\mathbf{w} = (w_1; w_2; ...; w_d)$, After the $\mathbf{w}$ and b are learned, the model is determined.

How to determine $\mathbf{w}$ and b? The key lies in how to measure the difference between $f(\mathbf{x})$ and y. Mean square error is the most commonly used performance metric in regression tasks, so we can try to minimize the mean square error, i.e.

$$(\mathbf{w}^*, b^*) = \arg\min_{(\mathbf{w},b)} \sum_{i=1}^{d} (f(x_i) - y_i)^2 \tag{5.3}$$

The method of solving model by minimizing the mean square error is called "least squares". In linear regression, the least squares method is trying to find a line that minimizes the sum of Euclidean distances of all samples to the line.

For the sake of discussion, we absorb $\mathbf{w}$ and b into vector form $\hat{\mathbf{w}} = (\mathbf{w}; b)$. Correspondingly, the attributes set is represented as a matrix $\mathbf{X}$ of size $m \times (d+1)$, in which each row corresponds to a sample, and the d elements of this row correspond to the d attribute values of this sample. The last element is always 1, i.e.

$$\mathbf{X} = \begin{pmatrix} x_{11} & x_{12} & \cdots & x_{1d} & 1 \\ x_{21} & x_{22} & \cdots & x_{2d} & 1 \\ \vdots & \vdots & \ddots & \vdots & \vdots \\ x_{m1} & x_{m2} & \cdots & x_{md} & 1 \end{pmatrix} = \begin{pmatrix} \mathbf{x}_1^T & 1 \\ \mathbf{x}_2^T & 1 \\ \vdots & \vdots \\ \mathbf{x}_m^T & 1 \end{pmatrix} \tag{5.4}$$

If we also rewrite the label as a vector $\mathbf{y} = (y_1; y_2; ...; y_m)$, then, similar to equation (5.3), we have

$$\hat{\mathbf{w}}^* = \arg\min_{\hat{\mathbf{w}}} (\mathbf{y} - \mathbf{X}\hat{\mathbf{w}})^T (\mathbf{y} - \mathbf{X}\hat{\mathbf{w}}) \tag{5.5}$$

Let $E_{\hat{\mathbf{w}}} = (\mathbf{y} - \mathbf{X}\hat{\mathbf{w}})^T (\mathbf{y} - \mathbf{X}\hat{\mathbf{w}})$, calculate the derivative of $E_{\hat{\mathbf{w}}}$ with respect to $\hat{\mathbf{w}}$, we can get

$$\frac{\partial E_{\hat{\mathbf{w}}}}{\partial \hat{\mathbf{w}}} = 2\mathbf{X}^T (\mathbf{X}\hat{\mathbf{w}} - \mathbf{y}) \tag{5.6}$$

Let the above equation equals to zero, we can obtain the closed-form solution of the optimal solution. When $\mathbf{X^T X}$ is a full-rank matrix or a positive definite matrix, let equation (5.6) equals to zero, we can get

$$\hat{\mathbf{w}}^* = (\mathbf{X}^T \mathbf{X})^{-1} \mathbf{X}^T \mathbf{y} \tag{5.7}$$

in which $(\mathbf{X}^T \mathbf{X})^{-1}$ is the inverse of matrix $(\mathbf{X}^T \mathbf{X})$. Let $\hat{\mathbf{x}}_i = (\mathbf{x}_i, 1)$, the final learned multiple linear regression model is

$$f(\hat{\mathbf{x}}_i) = \hat{\mathbf{x}}_i (\mathbf{X}^T \mathbf{X})^{-1} \mathbf{X}^T \mathbf{y} \tag{5.8}$$

5.2 Usability Analysis of Multiple Linear Regression

Whether multiple linear regression can be used in ocean wave prediction lies in whether the ocean wave prediction is a linear problem. If we simplify the oscillation mode of a certain point to a sine wave, we can find that there is a linear relationship between current wave height and future wave height, as shown in Figure 5.1 and Figure 5.2.

In Figure 5.1, there are two points of each color or shape. They represent a pair of wave height values, in which the previous point represents current wave height and the latter point represents future wave height (5 s later). Given that the wave period is 10 s and the wave height is 6 m, at 1 s, we measured the current wave height is 2.4271 m (i.e. the first yellow dot in Figure 5.1), so we predict that after 5 s (at 6 s), the wave height will be -2.4271 m (i.e. the second yellow dot in Figure 5.1). Another example is we measured that the current wave height is 0.9271 m (i.e. the first red triangle in Figure 5.1), so we predict that after 5 s (at 7 s), the wave height will be -0.9271 m (i.e. the second red triangle in Figure 5.1).

If we describe the relationship between current wave height and future wave height in another form, which take the current wave height as the x-axis and take the future wave height as the y-axis, the result shown in Figure 5.2 will be obtained.

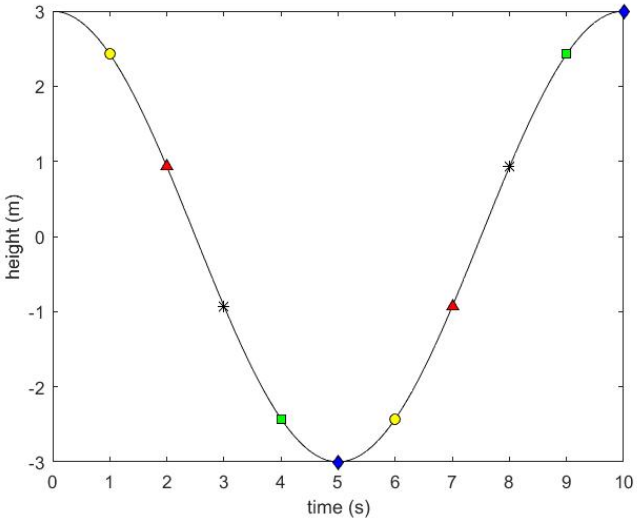

Figure 5.1 An Oscillation Curve of Sine Wave

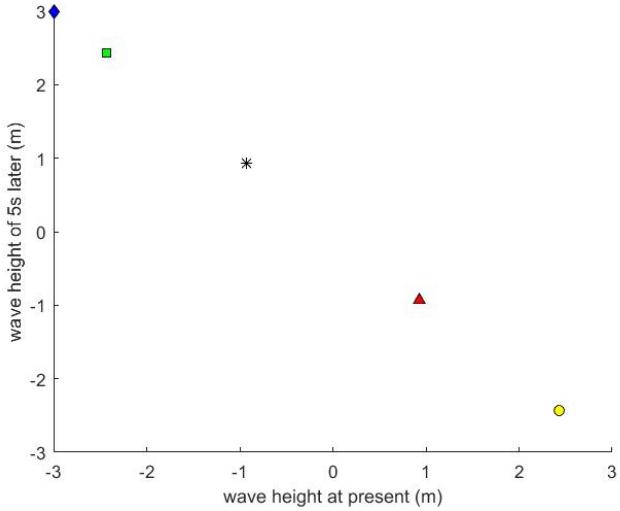

Figure 5.2 Linear Relationship between Current Wave Height and Future Wave Height

For example, the yellow dot in Figure 5.2 corresponds to the yellow dot in Figure 5.1. Its coordinates in Figure 5.2 are (2.4271, -2.4271), which means the current wave height of this point is 2.4271 m, and we can predict that the future wave height (after 5 s) of this point is -2.4271 m. From Figure 5.2, we can find that there is a linear relationship between current wave

height and future wave height. Therefore, multiple linear regression can be used to explore this linear relationship. The essence of this method is to find a line to fit most of data points in the graph.

Of course, the above situation is based on the premise that ocean wave oscillation is a simple sine wave, but the real ocean wave oscillation is not a simple sine wave, there will be some jitter on the micro level. So in real marine environment, the relationship between current wave height and future wave height will not be a simple straight line, but some messy data points distributed around the line, as shown in Figure 5.3. Thus, we can use multiple linear regression method to find the fitted line of these messy data points.

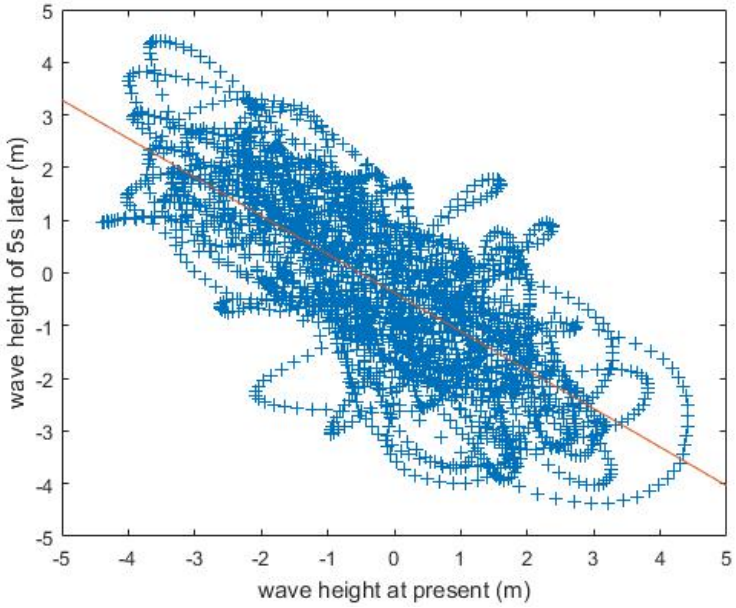

Figure 5.3 Real Relationship between Current Wave Height and Future Wave Height

5.3 Implementation Process

As mentioned in section 5.1, the linear model attempts to learn a function that predicts labels through a linear combination of attributes. Therefore, the $\mathbf{x}$ in equation (5.2) is the wave height of current period, and $f(\mathbf{x})$ is the future wave height that we want to predict. What we want to get is the weight matrix $\mathbf{w}$ and b. After getting the weight matrix, each time we get a new set of

current wave height data, we can multiply it with the weight matrix to get a set of data of future wave height.

Equation (5.7) has given the calculation method of weight matrix, we only need to calculate it through attribute matrix **X** (i.e. current wave height) and label *y* (i.e. future wave height). The construction method of matrix **X** and **y** is shown in Figure 5.4.

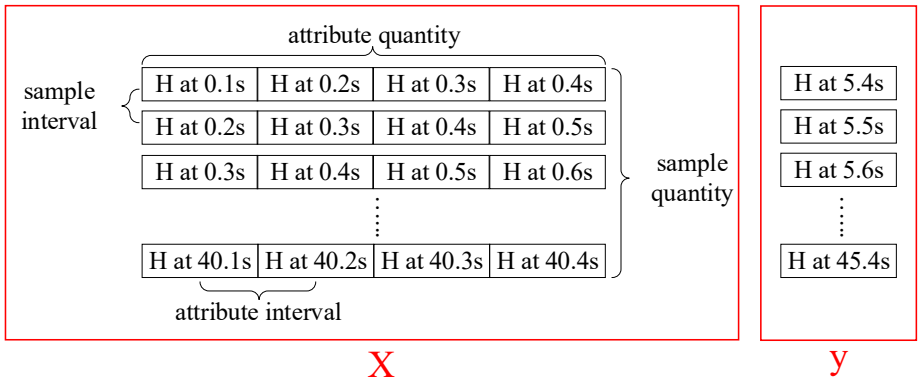

Figure 5.4 Construction Method of Matrix **X** and **y**

5.4 Experiment and Results Analysis

In this section, we firstly introduce the method of parameters selection in the experiment process, then show and analyse the experiment results. The effects of multiple linear regression method are affected by weight matrix. The construction method of weight matrix involves the selection of four parameters, which are sample quantity, sample interval, attribute quantity and attribute interval. The selection of these four parameters is described in section 5.4.1 and 5.4.2. The analysis of experiment results is described in section 5.4.3.

5.4.1 Parameter Setting

5.4.1.1 Selection of Sample Quantity and Sample Interval

We firstly set other parameters as shown in Table 5.1, then test the prediction accuracy of multiple linear regression method with different sample quantity and sample interval.

Table 5.1 Parameter Setting to Test Optimal Sample Quantity and Sample Interval

Parameter	Value
Wind speed	20m/s
Attribute interval	0.1s
Attribute quantity	5
Prediction time span	5s
Test start time	1005s
Test end time	1105s

By testing the prediction error with different sample quantity and sample interval, we obtained the results as shown in Figure 5.5. It can be seen that as the sample interval increases, the prediction error has a tendency of decreasing, but after decreasing to a certain extent, it does not continue to decrease, but fluctuates within a certain range. Similarly, as the sample quantity increases, the prediction error also tends to decrease firstly, and then fluctuates within a certain range.

Results show that when the sample quantity is 450 and the sample interval is 0.9s, the multiple linear regression method has the best prediction accuracy. It should be pointed out that the optimal values of sample quantity and sample interval are related to the parameters setting during experiment, which are not a unique determined value. When the experiment parameters (such as sea state) are changed, the optimal values should be re-measured. The significance of this subsection is providing a test method to determine the optimal value of sample quantity and sample interval, rather than providing a unique determined optimal value.

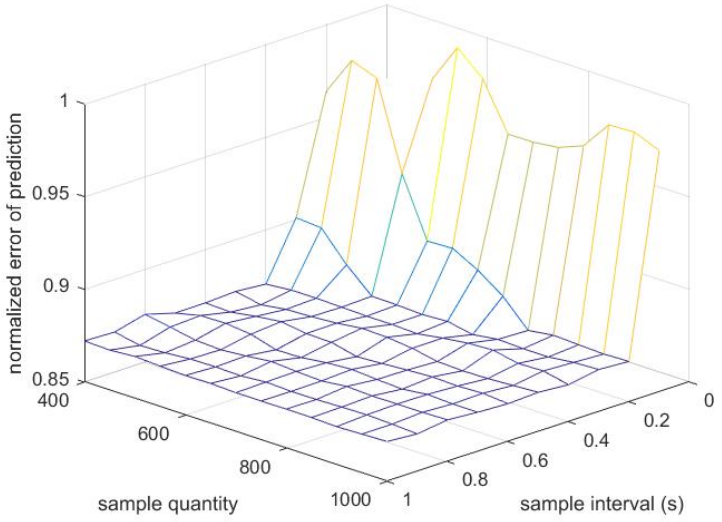

Figure 5.5 Prediction Error versus Sample Quantity and Sample Interval

5.4.1.2 Selection of Attribute Quantity and Attribute Interval

Similar to subsection 5.4.1, we select the attribute quantity and attribute interval with the parameters shown in Table 5.2.

Table 5.2 Parameter Setting to Test Optimal Attribute Quantity and Attribute Interval

Parameter	Value
Wind speed	20m/s
Sample interval	0.9s
Sample quantity	450
Prediction time span	5s
Test start time	500s
Test end time	600s

By testing the prediction error with different attribute quantity and attribute interval, we get the results shown in Figure 5.6. It can be seen from Figure 5.6, as the attribute interval increases, the

prediction error shows a fluctuating trend. As the attribute quantity increases, the prediction error shows a downward trend.

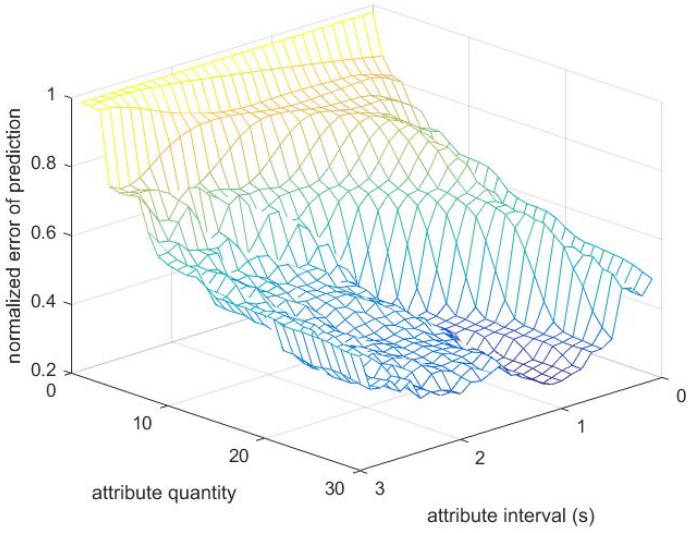

Figure 5.6 Prediction Error versus Attribute Quantity and Attribute Interval

Results show that when the attribute quantity is 30 and the attribute interval is 1.1s, the multiple linear regression method has the best prediction accuracy. Similar to subsection 5.4.1, the purpose of this subsection is also providing a test method to determine the optimal value of attribute quantity and attribute interval, rather than providing a unique determined optimal value.

5.4.2 Results and Analysis

5.4.2.1 Prediction Results for Simulated Ocean Wave

Figure 5.7 shows the results of ocean wave prediction based on multiple linear regression. The experiment parameters are set the same as Table 5.2. It can be seen from Figure 5.7, the predicted value and the real value are highly consist with each other except some slight difference in peak points.

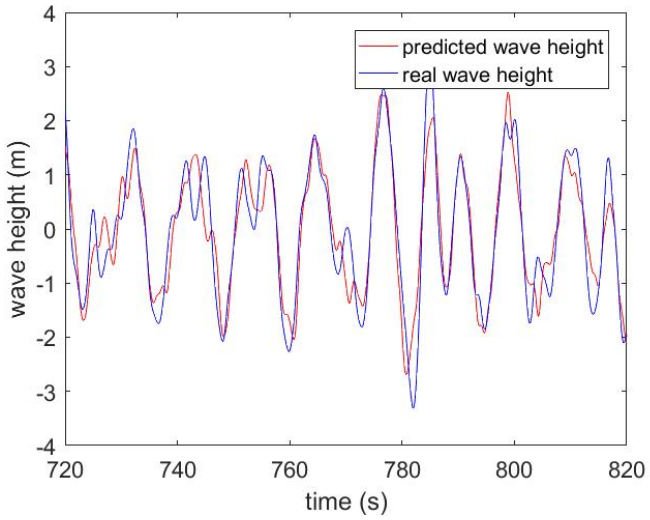

Figure 5.7 Prediction Results of Multiple Linear Regression

Figure 5.8 shows the prediction accuracy of the multiple linear regression method. The x-axis is the real value and the y-axis is the predicted value. If the data point is on the line y=x or close to this line, then it indicates that the prediction accuracy is high. By fitting the data points, we can get that the expression of the fitted line is $y = 0.8372 \times x - 0.0044$, which is very close to the line y=x, and the correlation coefficient R=0.9231, which indicates that the multiple linear regression method has a high prediction accuracy.

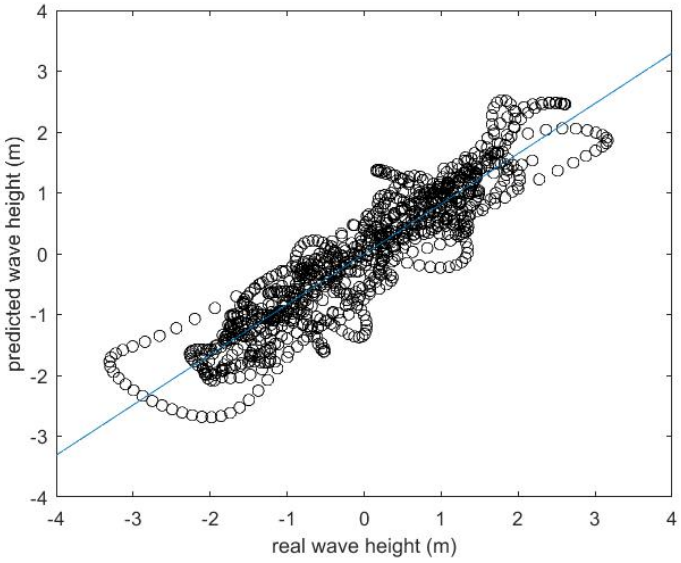

Figure 5.8 Prediction Accuracy of Multiple Linear Regression

Figure 5.9 compares the performance of multiple linear regression method with various neural network methods. It can be seen that the multiple linear regression method has the highest R value, i.e. the best prediction accuracy. It should be pointed out that although the multiple linear regression method proposed in this section has a better performance than the Elman neural network, this method can only be used in linear wave prediction, but the Elman neural network can be used in nonlinear wave prediction. These two methods cannot substitute each other. In addition, the computational complexity of multiple linear regression is significantly lower than other neural network methods, which can generate prediction results in a few seconds, while neural network methods usually require training processes of up to tens of seconds or even a few minutes.

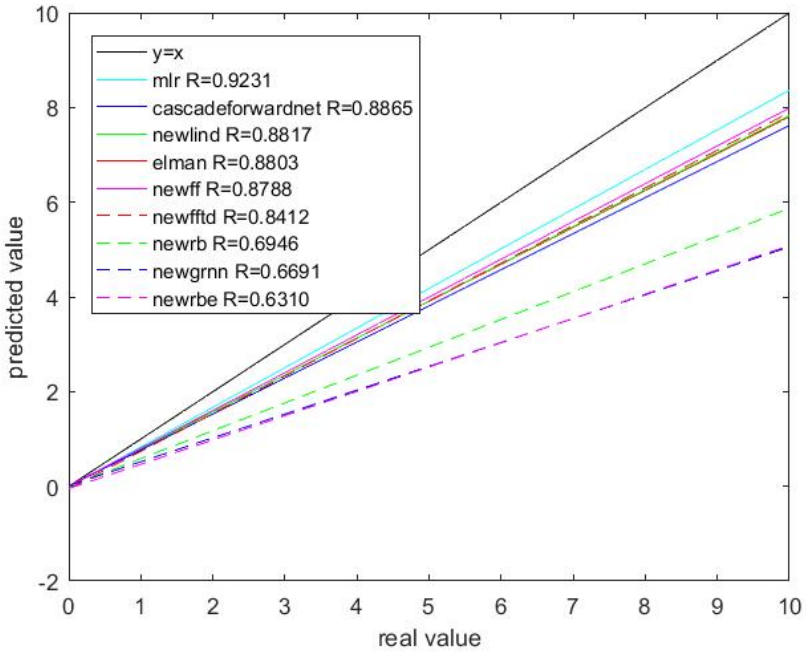

Figure 5.9 Performance Comparison of Various Methods

5.4.2.2 Prediction Results for Real Ocean Wave

Besides simulation experiment, we also used real ocean wave data to test our prediction method. Figure 5.10 shows the real ocean wave data which is from literature [Ryc97] and originally supplied by M. Olagnon, IFREMER, France and P. Palo, US Naval Facilities Engineering Service Center.

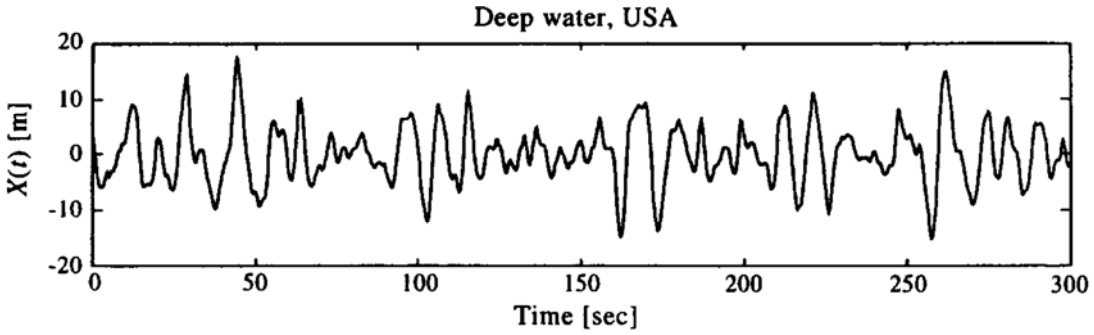

Figure 5.10 Real Ocean Wave Data

It is a kind of deep water wave as well as linear wave. We use the first 200 s data to train the neural network and the last 100 s data to test the neural network. The parameter selection process is similar to Subsection 5.4.1 and need not to be repeated here. We just show the prediction results.

Figure 5.11 shows the prediction results of multiple linear regression method and Figure 5.12 shows the correlation coefficient comparison of multiple linear regression method with other methods. It can be seen that the multiple linear regression method has the highest R value, which means it has the highest prediction accuracy.

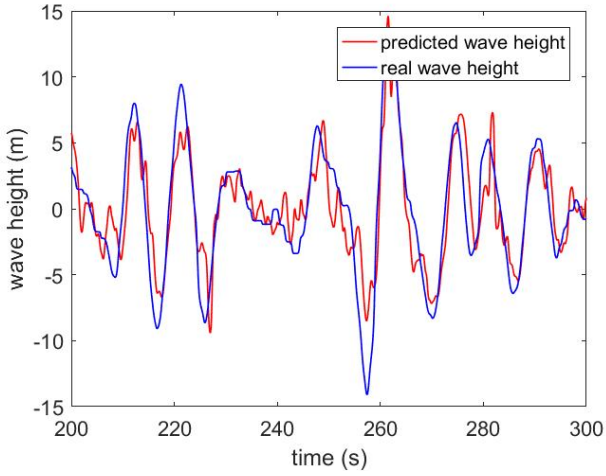

Figure 5.11 Prediction Results of Multiple Linear Regression

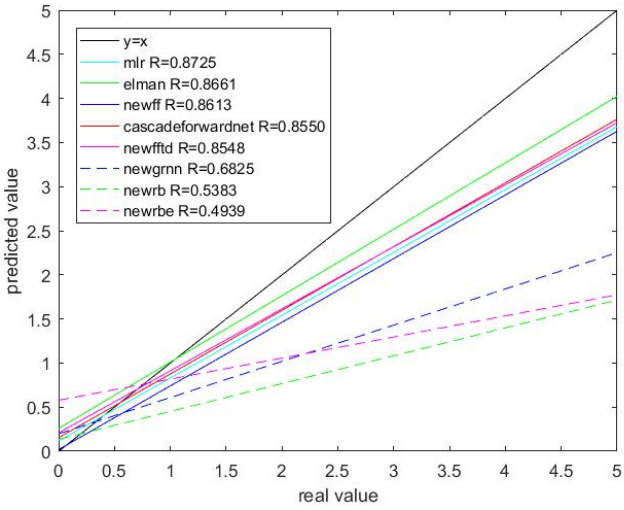

Figure 5.12 Correlation Coefficient Comparison of MLR with Other Methods

Figure 5.13 shows the comprehensive comparison of various methods. It can be seen that our multiple linear regression method has the best result in both evaluation systems, thus, it is an effective way to predict linear waves.

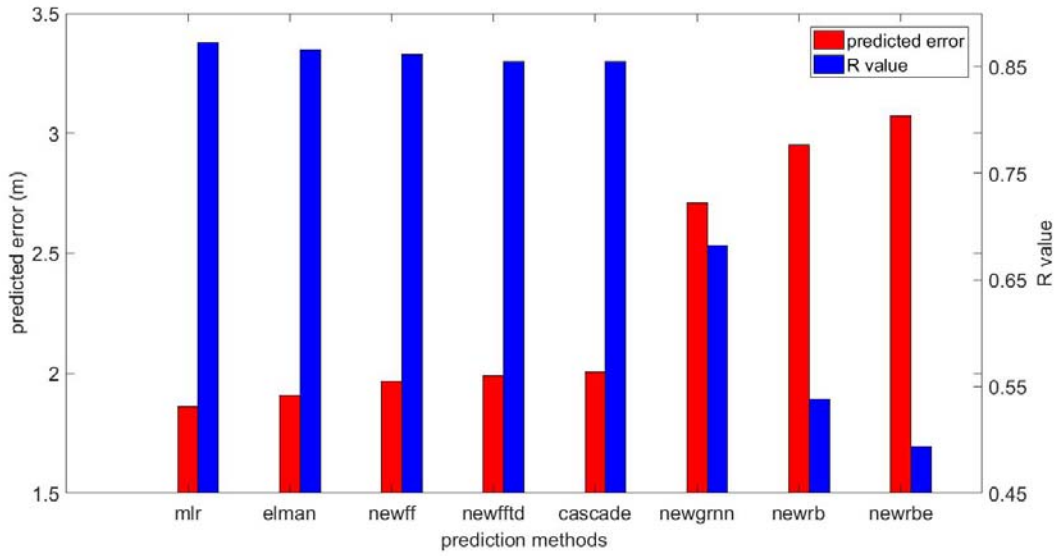

Figure 5.13 Comprehensive Comparison of Various Methods

5.4.3 Conclusion

In this Chapter, we conducted two sets of experiments. From the perspective of data sources, we tested our method with simulated data and real data respectively. Experiment Results show that our method has the highest prediction accuracy among various methods. In addition, by testing with simulated data and real data, we demonstrate that out method is effective in real marine environment.

To sum up, this Chapter proposed an effective technology for our future networking protocol design.

Chapter 6 Ocean Wave Simulation

So far, we can already measure and predict wave heights. But it is impossible to do every experiment in real marine environment during the process of our networking protocol design. We need a simulation platform of marine environment. In this chapter, we mainly introduce a spectrum-based ocean wave simulation method that proposed by Tessendorf [Tes01]. Before introducing this method, we firstly introduce an ocean wave simulation method called Gerstner Waves. This is because Tessendorf Waves are developed on the basis of Gerstner Waves, and Gerstner Waves is mathematically simpler than Tessendorf Waves. By explaining Gerstner Waves, we can introduce a number of oceanographic concepts to help readers understand Tessendorf Waves in subsequent process. After introducing Tessendorf Waves, we introduce an improved method for Tessendorf Waves which can make the simulation more realistic.

6.1 Gerstner Waves

Gerstner waves were first found as an approximate solution to the fluid dynamic equations almost 200 years ago [Tes01]. There first application in computer graphics is the work by Fournier and Reeves in 1986 [Fou86]. They describe the surface in terms of the motion of individual points on the surface. To a good approximation, points on the surface of the water go through a circular motion as a wave passes by [Tes01], as shown in Figure 6.1.

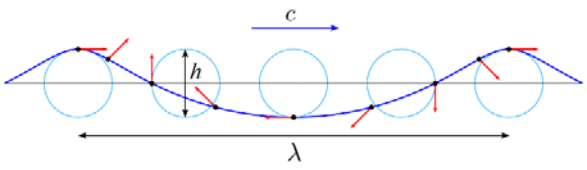

Figure 6.1 Motion of Individual Points on the Surface

If we only consider the motion in the XZ plane, the equations of the motion of a particle are [Fou86]:

$$\begin{cases} x(x_0,t) = x_0 + h\sin(kx_0 - \omega t) \\ z(x_0,t) = z_0 - h\cos(kx_0 - \omega t) \end{cases} \tag{6.1}$$

in which (x_0, z_0) is the rest position of a particle on the undisturbed surface, h is the wave amplitude, t is the current time, $k = 2\pi / \lambda$ is the wave number, $\omega = \sqrt{gk}$ is the angular velocity, g is the gravitational constant.

Figure 6.2 shows the various wave shapes obtained by different values of $k \times h$. When $k \times h = 0.2$, the shape is almost a sine wave. When $k \times h = 0.8$, the shape is a cycloid. The limiting reasonable value for $k \times h$ is 1, above which will lead to self-intersection so that the wave shape is not desirable and realistic.

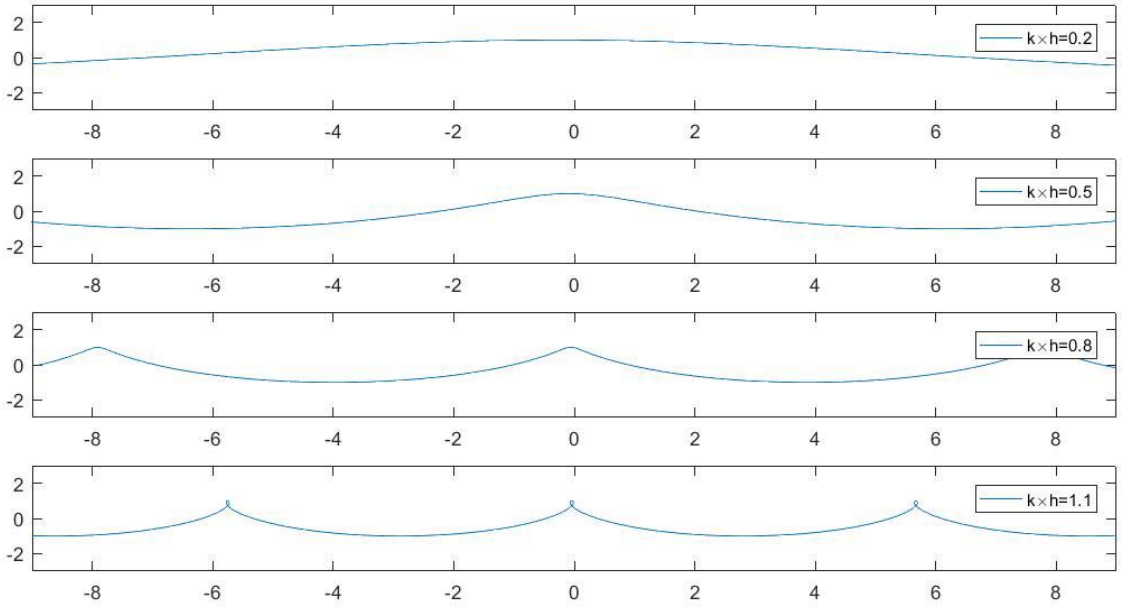

Figure 6.2 Wave Shapes with Different Parameters

Summing several waves and extending equation (6.1) to 2D surface, we obtained [Fre08]

$$\begin{cases} \mathbf{x}(\mathbf{x}_0, t) = \mathbf{x}_0 + \sum_{\mathbf{k}} \hat{\mathbf{k}} h_0(\mathbf{k}) \sin(\mathbf{k}\mathbf{x}_0 - \omega(k)t + \phi(\mathbf{k})) \\ z(\mathbf{x}_0, t) = z_0 - \sum_{\mathbf{k}} h_0(\mathbf{k}) \cos(\mathbf{k}\mathbf{x}_0 - \omega(k)t + \phi(\mathbf{k})) \end{cases} \tag{6.2}$$

in which $\mathbf{x} = (x, y)$ is the horizontal particle position at time t, $\mathbf{x}_0 = (x_0, y_0)$ is its position at rest, $\mathbf{k} = (k_x, k_y)$ is the wave vector with magnitude $|\mathbf{k}| = k$ and direction of the considered wave propagation, $\hat{\mathbf{k}} = \mathbf{k} / |\mathbf{k}|$ is the unit vector of $\mathbf{k}$, $\phi(\mathbf{k}) \in [0, 2\pi]$ is the initial phase.

Figure 6.3 shows an example with three waves in the set. Interesting and complex shapes can be obtained in this way [Tes01].

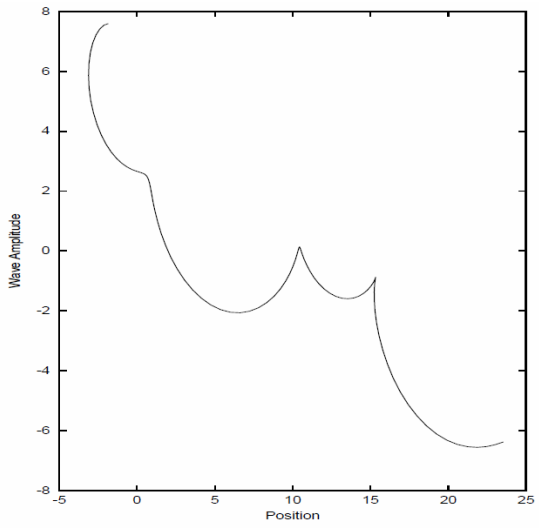

Figure 6.3 Example of Superposing Three Waves

6.2 Tessendorf Wave

As described in section 6.1, ocean waves are linearly superposed by waves of different amplitudes and different angular frequencies. Therefore, there are many calculation methods for equation (6.2). The simplest is to superpose directly, but this method is computationally inefficient. Tessendorf proposed an FFT-based (Fast Fourier Transform) calculation method, because the FFT can superpose a large number of unit waves efficiently and in real time. For a $N \times M$ ($N = 2^i, M = 2^j$, i, j are positive integers) complex set $F_{n,m}$, a complex set $F_{p,q}$ can be obtained by two-dimensional IFFT (Inverse Fast Fourier Transform):

$$F_{p,q} = \sum_{n=-N/2}^{N/2-1} \sum_{m=-M/2}^{M/2-1} F_{n,m} \exp(i2\pi(\frac{np}{N} + \frac{mq}{M})) \tag{6.3}$$

in which $p \in [-N/2, N/2-1]$, $q \in [-M/2, M/2-1]$.

In order to use the IFFT algorithm, we rewrite equation (6.2) as complex number form by Euler's formula:

$$\begin{cases} \mathbf{x}(\mathbf{x}_0,t) = \mathbf{x}_0 + I\left(\sum_{\mathbf{k}} \hat{\mathbf{k}} h(\mathbf{k},t)\exp(i\mathbf{k}\mathbf{x}_0)\right) \\ z(\mathbf{x}_0,t) = z_0 - R\left(\sum_{\mathbf{k}} h(\mathbf{k},t)\exp(i\mathbf{k}\mathbf{x}_0)\right) \end{cases} \tag{6.4}$$

in which $I(\ )$ and $R(\ )$ represent the imaginary and real part of the expression respectively, and

$$h(\mathbf{k},t) = h_0(\mathbf{k})\exp(i(-\omega(k)t + \phi(\mathbf{k}))) \tag{6.5}$$

The value of $\mathbf{x}_0$ is obtained by dividing the horizontal plane into $N \times M$ grids and obtain $N \times M$ sampling points. Therefore, $\mathbf{x}_0 = (nL_x / N, mL_y / M)$, in which n, m are integers and $n \in [-N/2, N/2-1]$, $m \in [-M/2, M/2-1]$.

According to equations (6.3), (6.4) and the expression of $\mathbf{x}_0$, we can find:

$$\begin{cases} \frac{nL_x}{N} \cdot k_x = 2\pi \frac{np}{N} \\ \frac{mL_y}{M} \cdot k_y = 2\pi \frac{mq}{M} \end{cases} \tag{6.6}$$

By solving the above equation, we can obtain $\mathbf{k} = (k_x, k_y) = (2\pi p / L_x, 2\pi q / L_y)$, in which $p \in [-N/2, N/2-1]$, $q \in [-M/2, M/2-1]$.

According to the expression of $\mathbf{k}$ and $\mathbf{x}_0$, we can transform equation (6.4) to

$$\begin{cases} \mathbf{x} = \mathbf{x}_0(p,q) + I\left(\sum_{n=-N/2}^{N/2-1}\sum_{m=-M/2}^{M/2-1} \hat{\mathbf{k}} h(\mathbf{k},t)\exp(i2\pi(\frac{np}{N} + \frac{mq}{M}))\right) \\ z = z_0 - R\left(\sum_{n=-N/2}^{N/2-1}\sum_{m=-M/2}^{M/2-1} h(\mathbf{k},t)\exp(i2\pi(\frac{np}{N} + \frac{mq}{M}))\right) \end{cases} \tag{6.7}$$

in which $\mathbf{x}_0(p,q) = (pL_x / N, qL_y / M)$, $\hat{\mathbf{k}} = (k_x / |\mathbf{k}|, k_y / |\mathbf{k}|)$.

For equation (6.7), as long as we know $h(\mathbf{k},t)$, we can use the IFFT algorithm to calculate the real time height z and horizontal coordinate $\mathbf{x}$ of each sample point at one time. It can be seen

from equation (6.5) that $h(\mathbf{k},t)$ is composed of three parts: amplitude $h_0(\mathbf{k})$, phase $\exp(-i\omega(k)t)$ and initial phase $\exp(i\phi(\mathbf{k}))$. Their expressions are as follows:

(1) Amplitude $h_0(\mathbf{k})$: Studies in fluid mechanics and oceanography have shown that the energy of a wave is proportional to the square of the amplitude, so the amplitude $h_0(\mathbf{k})$ can be obtained by calculating the square root of the wave spectrum. Tessendorf Wave uses the Phillips wave spectrum and its expression is:

$$P(\mathbf{k}) = A\frac{\exp(-1/(kL)^2)}{k^4}|\hat{\mathbf{k}}\cdot\mathbf{d}|^2 \tag{6.8}$$

in which $L = V^2/g$ is the largest possible waves arising from a continuous wind of speed V, **d** is the direction of the wind, A is a numeric constant.

(2) Phase $\exp(-i\omega(k)t)$: Each variable in this expression is the same as described in Section 6.1.

(3) Initial phase $\exp(i\phi(\mathbf{k}))$: A large number of ocean observation statistics show that the wave height of fully developed sea in open sea area approximately obeys the normal distribution, and its modulus obeys the Rayleigh distribution. Hereby, we use two independent normally distributed random number ξ_r and ξ_i (with mean 0, standard deviation 1) to replace the real part and imaginary part of $\exp(i\phi(\mathbf{k}))$ respectively, then $\sqrt{\xi_r^2+\xi_i^2}$ obeys the Rayleigh distribution, and the standard deviation is $\sqrt{2}$. To ensure the standard deviation of amplitude is 1, ξ_r and ξ_i are reduced $\sqrt{2}$ times respectively, i.e. $\exp(i\phi(\mathbf{k})) = \frac{1}{\sqrt{2}}(\xi_r + i\xi_i)$.

So far, equation (6.5) is transformed into

$$h(\mathbf{k},t) = \frac{1}{\sqrt{2}}(\xi_r + i\xi_i)\sqrt{P(\mathbf{k})}\exp(-i\omega(k)t) \tag{6.9}$$

As long as we input a constantly changing time *t*, an ocean wave animation can be generated by IFFT.

Since we only want to get the real number result when calculating the sea surface (i.e. when performing the IFFT), equation (6.5) can be rewritten as

$$h(\mathbf{k},t) = h_0(\mathbf{k})\exp(i(-\omega(k)t + \phi(\mathbf{k}))) + h_0^*(\mathbf{k})\exp(-i(-\omega(k)t + \phi(\mathbf{k}))) \quad (6.10)$$

in which * is the complex conjugate operator. Equation (6.10) satisfies the condition $h^*(\mathbf{k},t) = h(-\mathbf{k},t)$. Expressions that satisfy this condition can get real number results after IFFT, and the computation process is faster. The physical meaning of equation (6.10) is that two different waves are superposed, which does not affect the visual effect of simulated ocean waves, because the ocean waves are originally composed of numerous waves of different amplitudes and different frequencies.

Figure 6.4 shows the ocean wave generated by Tessendorf model.

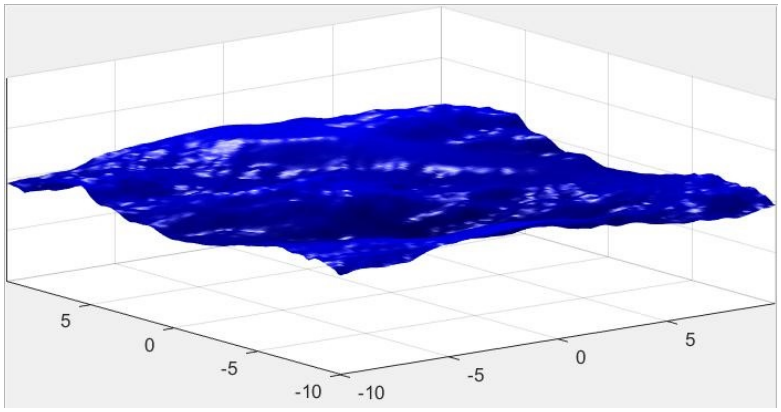

Figure 6.4 Tessendorf Waves

6.3 Revised Tessendorf Waves

The Tessendorf Waves just appear to match the oscillation characteristics of ocean waves, but the change of wave height with wind speed is not match with that of real marine environment. In this section, we propose a method to correct the wave height of the Tessendorf Wave, so as to make it more realistic.

In real marine environment, there is no strict mathematical relationship between average wave height and wind speed. When the wind speeds of two sea areas are the same, they may have different average wave heights; when the wind speeds of the two sea areas are different, they may have the same average wave height. The Beaufort Scale is a sea state grading method

recommended by the World Meteorological Organization. It describes the approximate relationship between average wave height and wind speed, as shown in Figure 6.5.

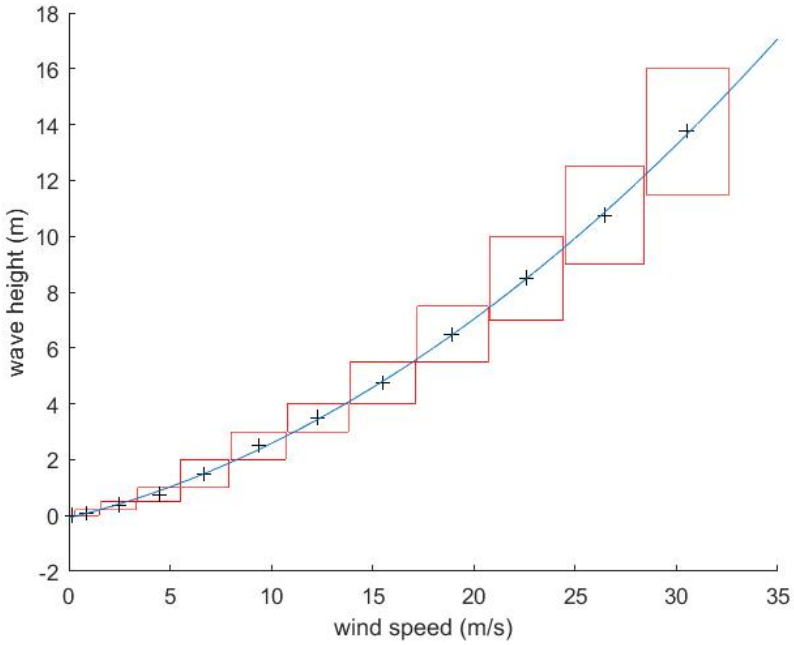

Figure 6.5 Beaufort Scale

The red blocks indicate the possible value range of average wave height versus the corresponding change interval of wind speeds. For example, the rightmost red block indicates that when the wind speed is 28.5-32.6 m/s, the average wave height may be any value between 11.5-16 m. We fit the midpoint coordinates of each block and get a curve that roughly represents the mathematical relationship between wind speed and average wave height, as the blue curve shown in Figure 6.5, and its expression is:

$$h = 0.009s^2 + 0.1769s - 0.0827 \tag{6.11}$$

However, the relationship between wave height and wind speed in Tessendorf waves doesn't follow above rules. Figure 6.6 shows the relationship of them in Tessendorf waves. Put aside the value of Y axis and just consider the shape of the curve, it can be seen that there is a big difference between Figure 6.6 and Figure 6.5. Thus, Tessendorf waves should be revised.

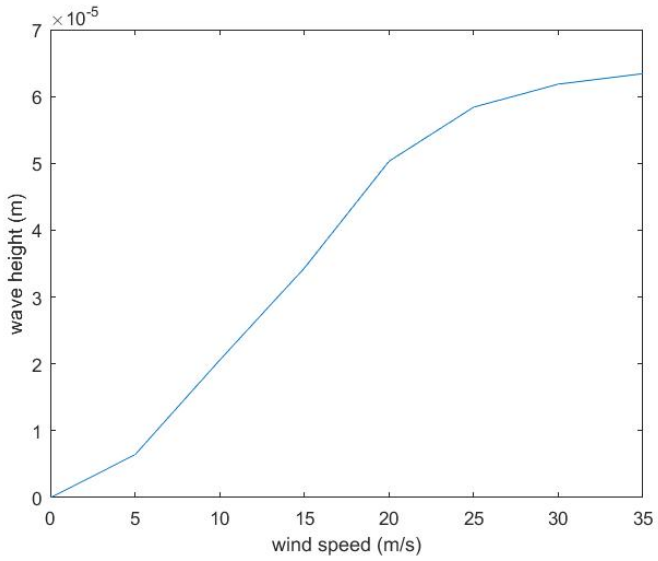

Figure 6.6 Tessendorf's Wave Height versus Wind Speed

In our thesis, when conducting simulation, we firstly calculate the wave height that it should be in real marine environment, then measure the average wave height that generated by Tessendorf wave. Finally, we convert the Tessendorf's wave height to real wave height by amplifying them proportionally.

Chapter 7 Conclusion

In this thesis, we have solved three problems in development of marine mesh network, they are ocean wave measurement, ocean wave prediction and ocean wave simulation.

In chapter 3, we proposed an accelerometer-based wave measurement method. It can measure the displacement by calculating the double integration of acceleration. It neither requires to install additional mechanical structures, nor requires to use expensive laser rangefinders. Thus, it is a kind of cheap and feasible solution to measure real time wave height. Experiment results show that it has an excellent measurement accuracy.

In chapter 4, we implemented a neural-network-based ocean wave prediction method for nonlinear waves. It can predict the oscillation mode of ocean waves accurately. Experiment results show that its prediction accuracy is higher than other neural network methods. Thus, it is an effective technology to improve network throughput and reduce energy consumption.

In chapter 5, we implemented a multiple-linear-regression-based ocean wave prediction method for linear waves. It can predict the oscillation mode of linear wave accurately. Experiment results show that its prediction accuracy is higher than other prediction methods, and its time consumption of prediction is significantly lower than other prediction methods. Thus, it is also an effective technology to improve network throughput and reduce energy consumption.

In chapter 6, we implemented a spectrum-based ocean wave simulation method. This method can simulate the movement of ocean waves realistically and in real time. Thus, it can provide a test platform for our future network protocol design as well as data support for our ocean wave prediction methods in chapter 4 and 5.

For future work, we plan to design the network protocol based on our simulation platform.

Bibliography

[Aur08] L. Auria, R. A. Moro, "Support Vector Machines (SVM) as a Technique for Solvency Analysis," *DIW Berlin Discussion Paper*, no. 811, 2008.

[Fou86] A. Fournier, W. T. Reeves, "A Simple Model of Ocean Waves," *in Proceedings of the 13th Annual Conference on Computer Graphics and Interactive Techniques (ACM SIGGRAPH)*, 1986, pp. 75-84.

[Fre08] J. Frechot, "Realistic Simulation of Ocean Surface using Wave Spectra," *in Proceedings of the 1st International Conference on Computer Graphics Theory and Applications (GRAPP)*, 2006, pp.76-83.

[Fro10] P. J. From, J. T. Gravdahl, P. Abbeel, "On the Influence of Ship Motion Prediction Accuracy on Motion Planning and Control of Robotic Manipulators on Seaborne Platforms," *in Proceedings of the IEEE International Conference on Robotics and Automation*, 2010, pp. 5281-5288.

[Fu10] H. Fu, S. Liu, F. Sun, "Ship Motion Prediction based on AGA-LSSVM," *in Proceedings of the 2010 IEEE International Conference on Mechatronics and Automation*, 2010, pp. 202-206.

[Fu15] H. Fu, Y. Wang, H. Zhang, "Ship Rolling Motion Prediction based on Extreme Learning Machine," *in Proceedings of the 34th Chinese Control Conference (CCC)*, 2015, pp. 3468-3472.

[Ge16] M. Ge, E. C. Kerrigan, "Short-term Ocean Wave Forecasting Using an Autoregressive Moving Average Model," *in Proceedings of the 11th International Conference on Control*, 2016.

[Ge17] Y. Ge, M. Qin, Q. Niu, "Prediction of Ship Motion Attitude based on BP Network," *in Proceedings of the 29th Chinese Control And Decision Conference (CCDC)*, 2017, pp. 1596-1600.

[Gir10] J. M. Giron-Sierra, J. F. Jimenez, "State-of-the-Art of Wave Measurement for Ship Motion Prediction," *in Proceedings of the 8th IFAC Conference on Control Applications in Marine Systems*, 2010, pp. 295-300.

[Gon00] J.-C. Gonzato, B. L. Saec, “On Modelling and Rendering Ocean Scenes,” *The Journal of Visualization and Computer Animation*, vol. 11, pp. 27-37, 2000.

[Gon08] J.-C. Gonzato, T. Arcila, B. Crespin, “Virtual Objects on Real Oceans,” *in Proceedings of the 18th International Conference on Computer Graphics (GRAPHICON)*, 2008 , pp. 49-54.

[Gop15] D. I. Gopinatha, G. S. Dwarakishb, “Wave Prediction using Neural Networks at New Mangalore Port along West Coast of India,” *in Proceedings of International Conference on Water Resources, Coastal and Ocean Engineering (ICWRCOE)*, 2015, pp. 143-150.

[Hu06] Y. Hu, L. Velho, X. Tong, B. Guo, H. Shum, “Realistic, Real-Time Rendering of Ocean Waves,” *Journal of Computer Animation and Virtual Worlds - Game Technologies*, vol. 17, pp. 59-67, 2006.

[Kal] https://en.wikipedia.org/wiki/Kalman_filter

[Kas90] M. Kass, G. Miller, “Rapid, Stable Fluid Dynamics for Computer Graphics,” *in Proceedings of the 17th Annual Conference on Computer Graphics and Interactive Techniques (ACM SIGGRAPH)*, 1990, pp. 49-57.

[Kha05] A. Khan, C. Bil, K. E. Marion, “Ship Motion Prediction for Launch and Recovery of Air Vehicles,” *in Proceedings of OCEANS*, 2005, pp. 2795-2801.

[Kha16] A. A. Khan, K. E. Marion, C. Bil, M. Simic, “Motion Prediction for Ship-Based Autonomous Air Vehicle Operations,” *Intelligent Interactive Multimedia Systems and Services 2016, Smart Innovation, Systems and Technologies*, vol. 55, pp. 323-333, 2016.

[Kuc11] S. Kuchler, J. K. Eberharter, K. Langer, K. Schneider, O. Sawodny, “Heave Motion Estimation of a Vessel Using Acceleration Measurements,” *in Proceedings of the 18th International Federation of Automatic Control (IFAC)*, 2011, pp. 14742-14747.

[Li16] Z. Li, J. Dong, Z. Song, H. Zhang, Y. Guo, “Prediction of Ship Roll Motion based on Combination of Phase Space Reconstruction Theory and Elman Network,” *in Proceedings of the IEEE International Conference on Information and Automation (ICIA)*, 2016, pp. 686-689.

[Lin] https://en.wikipedia.org/wiki/Linear_regression

[Lin11] Z. Lin, Q. Yang, Z. Guo, X. Li, “An Improved Real Time AR Method for the Surface Vessel Motion Prediction,” *in Proceedings of the 4th International Conference on Intelligent Networks and Intelligent Systems*, 2011, pp. 49-52.

[Lu14] K. Lu, N. Cheng, Q. Li, “Research and Simulation on the Carrier Deck Motion Adaptive Prediction for ACLS Design,” *in Proceedings of 2014 IEEE Chinese Guidance, Navigation and Control Conference*, 2014, pp. 1341-1345.

[Luo14] W. Luo, W. Cai, “Modeling of Ship Manoeuvring Motion using Optimized Support Vector Machines,” *in Proceedings of the 5th International Conference on Intelligent Control and Information Processing*, 2014, pp. 476-478.

[Luo16] W. Luo, J. Ren, “On the Identification of Coupled Pitch and Heave Motions using Support Vector Machine,” *in Proceedings of the 28th Chinese Control and Decision Conference (CCDC)*, 2016, pp. 3316-3321.

[Mas87] G. A. Mastin, P. A. Watterberg, J. F. Mareda, “Fourier Synthesis of Ocean Scenes,” *IEEE Computer Graphics and Applications (IEEE CG&A)*, vol. 7, pp. 16-23, 1987.

[Mas11] G. De Masi, F. Gaggiotti, R. Bruschi, M. Venturi, “Ship Motion Prediction by Radial Basis Neural Networks,” *in Proceedings of the IEEE Workshop On Hybrid Intelligent Models And Applications*, 2011.

[Min05] J. H. Mina, Y.-C. Lee, “Bankruptcy Prediction using Support Vector Machine with Optimal Choice of Kernel Function Parameters,” *Expert Systems with Applications*, vol. 28, pp. 603-614, 2005.

[Mit05] J. L. Mitchell, “Real-Time Synthesis and Rendering of Ocean Water,” *ATI Research Technical Report*, 2005.

[Msi07] I. S. Msiza, F. V. Nelwamondo, T. Marwala, “Artificial Neural Networks and Support Vector Machines for Water Demand Time Series Forecasting,” *in Proceedings of the IEEE International Conference on Systems, Man and Cybernetics*, 2007, pp. 638-643.

[Mul12] B. Muller, J. Reinhardt, M. T. Strickland, “Neural Networks: an Introduction,” *Springer Science & Business Media*, 2012.

[Nie13] M. B. Nielsen, A. Soderstrom, R. Bridson, “Synthesizing Waves from Animated Height Fields,” *ACM Transactions on Graphics (ACM TOG)*, vol. 32(1), article 2, 2013.

[Pea86] D. R. Peachey, “Modeling Waves and Surf,” *in Proceedings of the 13th Annual Conference on Computer Graphics and Interactive Techniques (ACM SIGGRAPH)*, 1986, pp. 65-74.

[Pen06] X. Peng, X. Zhao, L. Xu. “Real-time Prediction Algorithm Research of Ship Attitude Motion based on Order Selection with Corner Condition,” *in Proceedings of the 1st International Symposium on Systems and Control in Aerospace and Astronautics*, 2006, pp. 1070-1075.

[Pen15] X. Peng, B. Zhang, L. Rong, “Ship Motion Prediction of Combination Forecasting Model based on Adaptive Variable Weight,” *in Proceedings of the 34th Chinese Control Conference (CCC)*, 2015, pp. 4015-4019.

[Pen17] X. Peng, H. Dong, B. Zhang, “Echo State Network Ship Motion Modeling Prediction based on Kalman Filter,” *in Proceedings of 2017 IEEE International Conference on Mechatronics and Automation (ICMA)*, 2017, pp. 95-100.

[Per10] L. P. Perera, C. G. Soares, “Ocean Vessel Trajectory Estimation and Prediction Based on Extended Kalman Filter,” *in Proceedings of the 2nd International Conference on Adaptive and Self-adaptive Systems and Applications*, 2010, pp. 14-20.

[Pie64] W. J. Pierson, L. Moskowitz, “A Proposed Spectral Form for Fully Developed Wind Seas Based on the Similarity Theory of S. A. Kitaigorodskii,” *Journal of Geophysical Research*, vol. 69, pp. 5181-5190, 1964.

[Pre00] S. Premoze, M. Ashikhmin, “Rendering Natural Waters,” *in Proceedings of the 8th Pacific Conference on Computer Graphics and Applications (IEEE CG&A)*, 2000, pp. 23-30.

[Pui14] A. Puig-Centelles, F. Ramos, O. Ripolles, M. Chover, M. Sbert, “View-Dependent Tessellation and Simulation of Ocean Surfaces,” *The Scientific World Journal*, vol. 2014, article id. 979418, 2014.

[Rad13] K. Radhakrishnan, “A Kalman Filter based Sway Velocity Estimation for Rudder Roll Control of Ships,” *The International Journal of Computer Applications*, vol. 63, no. 5, pp. 2013.

[Rea] http://fortune.com/2014/06/20/five-surprising-reasons-ships-need-internet-access/

[Ryc97] I. Rychlik, P. Johannesson, M. R. Leadbetter, Modelling and Statistical Analysis of Ocean-wave Data Using Transformed Gaussian Processes, Marine Structures, vol. 10, pp. 13-47, 1997.

[Sat] http://www.globalmarinenet.com/satellite-internet-at-sea-hardware-airtime-and-pricing/

[Tes01] J. Tessendorf, "Simulating Ocean Water," *ACM SIGGRAPH Course Note*, 2001.

[Thu07] N. Thurey, M. Muller-Fischer, S. Schirm, M. Gross, "Real-time Breaking Waves for Shallow Water Simulations," *in Proceedings of the 15th Pacific Conference on Computer Graphics and Applications (IEEE CG&A)*, 2007, pp. 39-46.

[Tri81] M. Triantafyllou, M. Athans, "Real Time Estimation of the Heaving and Pitching Motions of a Ship, Using a Kalman Filter," *in Proceedings of OCEANS*, 1981, pp. 1090-1095.

[Tri82] M. Triantafyllou, M. Bodson, M. Athans, "Real Time Estimation and Prediction of Ship Motions using Kalman Filtering Techniques," *in Proceedings of the 14th Annual Offshore Technology Conference*, 1982, pp. 159-165.

[Tri83] M. Triantafyllou, M. Bodson, M. Athans, "Real Time Estimation of Ship Motions using Kalman Filtering techniques," *IEEE Journal of Oceanic Engineering*, vol. 8, pp. 9-20, 1983.

[Ts'o87] P. Y. Ts'o, B. A. Barsky, "Modeling and Rendering Waves: Wave-tracing using Beta-splines and Reflective and Refractive Texture Mapping," *ACM Transactions on Graphics (ACM TOG)*, vol. 6, pp. 191-214, 1987.

[Wan15] W. Wang, S. Qin, W. Wu, J. Zheng, "Prediction of Ship Pitch motion by Dual Autoregressive Model," *in Proceedings of the 27th Chinese Control and Decision Conference*, 2015, pp. 4846-4849.

[Yan08] X. Yang, H. Pota, M. Garratt, V. Ugrinovskii, "Ship Motion Prediction for Maritime Flight Operations," *in Proceedings of the 17th International Federation of Automatic Control (IFAC)*, 2008, pp. 12407-12412.

[Yan15] L. Yang, J. Zhang, Z. Yang, “Intelligent Prediction for Ship Motion based on Decomposition Strategy,” *in Proceedings of the 2015 IEEE International Conference on Mechatronics and Automation (ICMA)*, 2015, pp. 566-571.

[Zha14] W. Zhang, Z. Liu, “Real-Time Ship Motion Prediction Based on Time Delay Wavelet Neural Network,” *Journal of Applied Mathematics*, vol. 2014, article id. 176297, 2014.

[Zho10] B. Zhou, A. Shi, “LSSVM and Hybrid Particle Swarm Optimization for Ship Motion Prediction,” *in Proceedings of 2010 International Conference on Intelligent Control and Information Processing*, 2010, pp. 183-186.